DOCKET NO. 70-459

REGULATORY FILE CY.

Battelle
Columbus Laboratories
505 King Avenue
Columbus, Ohio 43201
Telephone (614) 299-3151
Telex 24-5454

June 19, 1972

RECEIVED
JUN 21 1972
U.S. ATOMIC ENERGY COMMISSION
Regulatory Mail Section

Mr. Charles E. MacDonald, Chief
Transportation Branch
Directorate of Licensing
U. S. Atomic Energy Commission
Bethesda, Maryland 20545

Dear Mr. MacDonald:

Letter March 10, 1972, from Donald A. Nussbaumer to Nuclear Reactor Laboratory, University of Arizona, Attention Dr. Monte V. Davis, requesting additional information for request for authorization to transport TRIGA fuel assemblies in the Battelle Model No. BMI-1 shipping cask, January 13, 1972.

In response to the referenced request we are submitting the attached information as Supplement No. 1.

Very truly yours,

Elmer C. Lusk

Elmer C. Lusk
Associate Fellow
Thermal Systems Division

ECL:aw

cc: Dr. Monte V. Davis
University of Arizona

DOCKETED
USAEC
JUN 23 1972
REGULATORY
MAIL SECTION
DOCKET CLERK

FROM:
Battelle
Columbus, Ohio
Mr. E. C. Lusk

TO:
MacDonald

CLASSIF: U

POST OFFICE

REG. NO:

DESCRIPTION: (Must Be Unclassified)
Ltr. Trans. Supplemental information to request for authorization to transport TRIGA fuel assemblies in the Batelle BMI-1 shipping cask....

ENCLOSURES:
Supplement No. 1

REMARKS:
This submittal is from Battelle in Behalf of University of Arizona

DATE OF DOCUMENT:	DATE RECEIVED	NO.:
06-19-72	06-21-72	3419

LTR.	MEMO:	REPORT:	OTHER:
X			

ORIG.:	CC:	OTHER:
1		

ACTION NECESSARY ☐	CONCURRENCE ☐	DATE ANSWERED:
NO ACTION NECESSARY ☐	COMMENT ☐	BY:

FILE CODE:
Docket No. 70-459

REFERRED TO	DATE	RECEIVED BY	DATE
MacDonald	6-23		
1 Reg. File Cy. & Folder			
1 PDR			
2 Extras			
Distribution			
2 RO			
X			
		3419	

File 70-459

DO NOT REMOVE
ACKNOWLEDGED

U.S. ATOMIC ENERGY COMMISSION

MAIL CONTROL FORM FORM AEC-326S (8-60)

☆ U.S. GOVERNMENT PRINTING OFFICE: 1971-424-962

RECEIVED
JUN 21 1972

SUPPLEMENT NO. 1

to

REQUEST FOR LICENSE TO TRANSPORT IRRADIATED TRIGA FUEL IN BMI-1 SHIPPING CASK

June 15, 1972

BATTELLE
Columbus Laboratories
505 King Avenue
Columbus, Ohio 43201

3419

SUPPLEMENT NO. 1

to

REQUEST FOR LICENSE TO TRANSPORT IRRADIATED
TRIGA FUEL IN BMI-1 SHIPPING CASK

June 15, 1972

INTRODUCTION

In a letter dated March 10, 1972, additional information was requested by the Division of Material Licensing to support the request by the University of Arizona to transport TRIGA fuel assemblies in the BMI-1 shiping cask. The BMI-1 cask has previously been licensed and the license application concerned the use of a Fuel Shipping Assembly (fuel can) to hold the TRIGA fuel assemblies in the cask during transport. The request for additional information concerned substantiation of the fuel can integrity in the event of the 30-ft free fall hypothetical accident, confirmation in the use of specific sealant materials and a request for a copy of the report upon which the criticality analyses were based.

RESPONSE TO SPECIFIC QUESTIONS

In a telephone conversation with the DML reviewer clarification was obtained of the specific questions underlying some of the items noted in the request for additional information. It was noted that for the 30-ft free fall incident, the cask impact forces calculated by DML during their review differ slightly from those presented in the Safety Analysis Report for the cask. For the purpose of consistency, the impact forces determined by DML are used in this response. They are presented in Table 1. It should be noted that the impact forces presented in Table 1 are those calculated to exist at the outer surface of the cask in the region of impact. No credit is taken for energy attenuation through the walls of the cask and at the interface of the cask cavity and the fuel can. This conservative approach is taken since the exact degree of attenuation cannot be accurately predicted.

TABLE 1. IMPACT FORCES USED IN ANALYSES FOR FUEL CAN INTEGRITY

Orientation	Impact Force, G
End Fall, on top	87.5
End Fall, on bottom	368
Side Fall	400
Corner (oblique)	153

1. Top End Impact

The cover plate of the fuel can has been modified as shown on the attached University of Arizona drawing, Sheet 1020, Revision A. A solid ring of rectangular cross section has been added at the outer edge of the cover to support the edge of the cover in the event of a top impact. Since the ring thickness is the same as the head of the draw bolt, the bolt and the ring will strike the end of the cavity simultaneously in the event of a top end impact. In order to evaluate the stresses on the fuel can in the event of a top end fall incident, the can was modeled and analyzed with the aid of a computer program, MONSA (Multilayer Orthotropic Nonsymmetric Shell Analysis), used by the Applied Solid Mechanics Division at Battelle. This program, based on the work of Dr. A. Kalnins, is discussed briefly in Appendix A. A paper by Dr. Kalnins which is the basis for the computer program is also included in Appendix A.

The can is sketched in Figure 1 and the model used in the analyses for the top end impact incident is presented in Figure 2. Because of the massiveness of the anchor nut relative to the thickness of the bottom, a fully fixed condition was assumed for the can bottom at the location of the anchor nut. The stresses in the can bottom and walls were analyzed by superimposing the effect of the static load of the draw bolt and the inertia load of the can and comparing the result with the effect of the static load and inertia load of the draw bolt. A seal load of 10 lb per inch is usually considered adequate for the type of seal used on the fuel can.

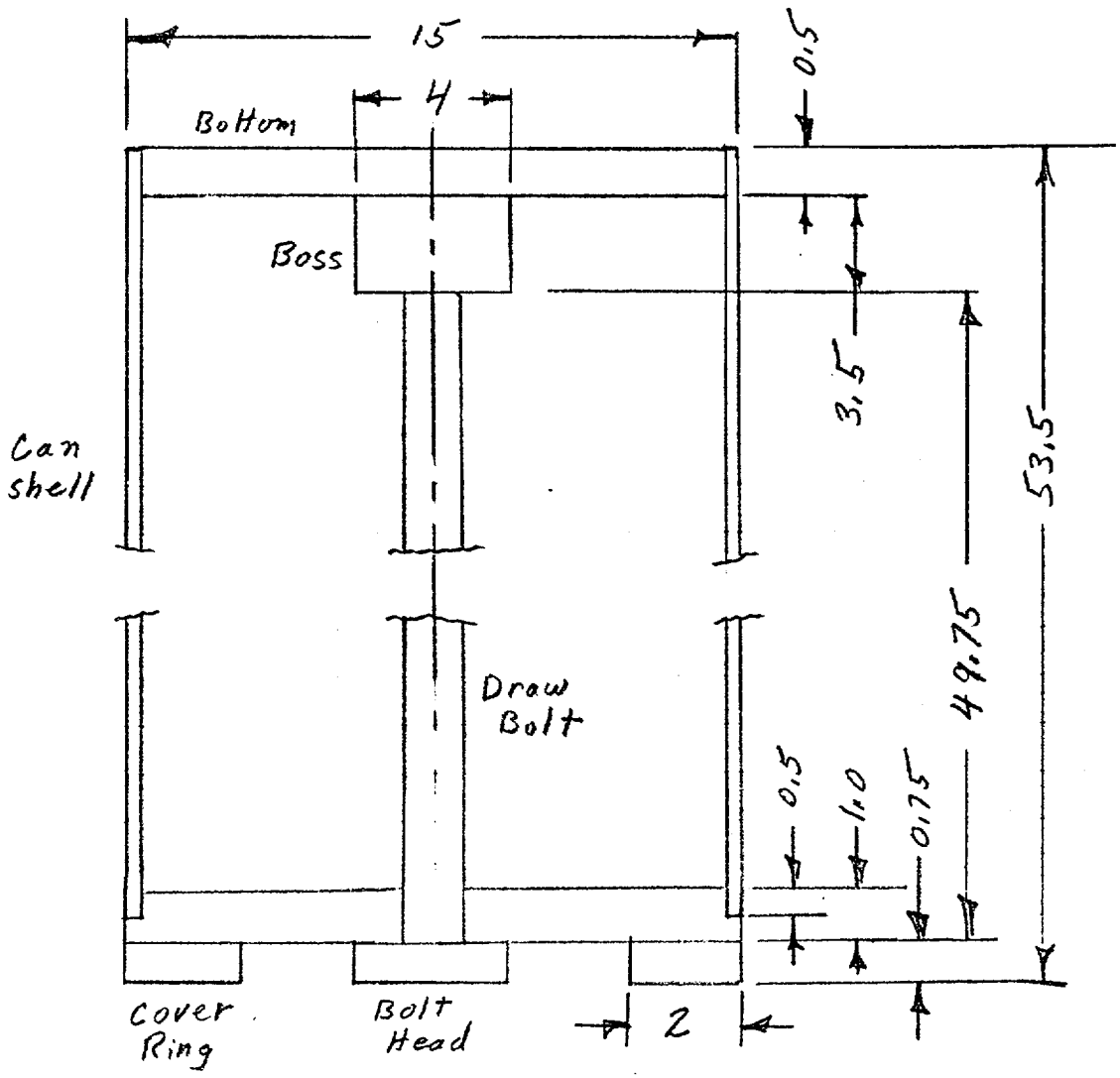

FIGURE 1. SKETCH OF FUEL CAN FOR THE TRANSPORT OF TRIGA FUEL ASSEMBLIES

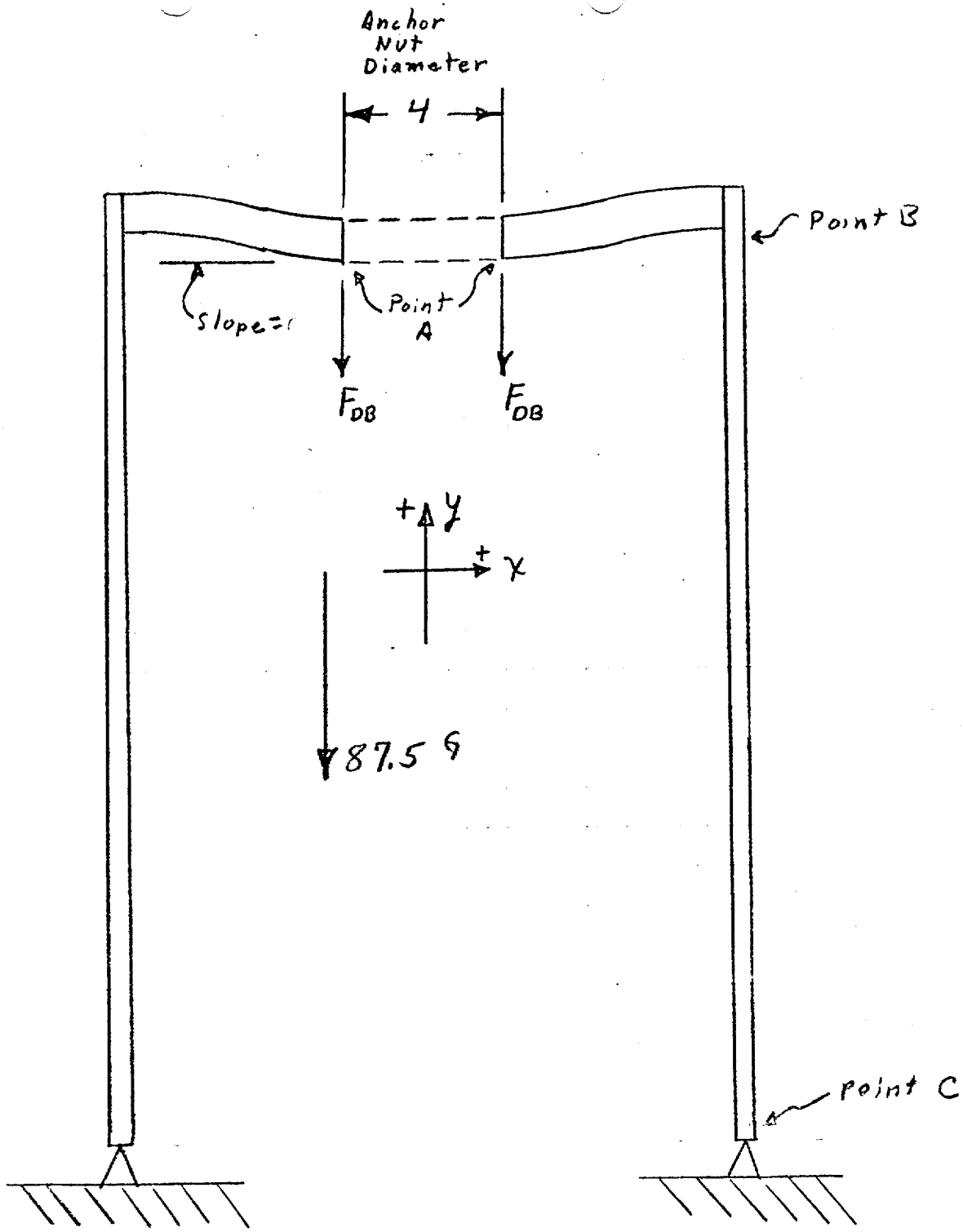

Boundry Conditions

At Pt. A Displacement $x = 0$
Slope $= 0$

At Pt C Displacement y = Displacement $x = 0$
Moment $= 0$

FIGURE 2. MODEL OF FUEL CAN FOR TOP END FALL ORIENTATION

However, as an extra assurance factor a seal load of 20 lb per inch has been selected. This would require a draw bolt tensile load of 945 lb. The operations manual was revised to indicate that the bolt should be tightened to a torque of 22 ft lb which will result in about 1,000 lb tensile load in the bolt (~21 lb per inch seal load).

The MONSA program was first run for the static condition, i.e., the effect of the 1,000 lb normal draw bolt load on the can. The results are summarized in Table 2. Under an impact condition, the inertial load of the anchor nut and bolt might either increase the load on the can or decrease it depending on the relative deformation between the can and the bolt. It is noted in Table 2 that for the 1,000 lb static condition the deformation of the can bottom at Point A is 0.00433. The MONSA computer program was then run to evaluate the effect of the inertia load of the can bottom and walls on the stresses in the can. As shown in Table 2, the can bottom at Point A would deflect 0.00607 inches if unsupported by the draw bolt. The total deformation then would be 0.01040 inches.

The deformation of the bolt under static and impact load can be calculated by the relation

$$e = \epsilon L = \frac{\sigma}{E} = \frac{F\ L}{A\ E}$$

where

e = total deformation of bolt, inches

ϵ = unit strain

σ = stress in the bolt

E = Young's Modulus = $29(10^6)$ psi

L = length of the bolt = 49.75 inches

F = static force of 1,000 lb or impact force at 87.5 G, lb

A = area of the 1-1/4 OD x 1/4 wall bolt = 0.7854 sq in.

g = impact force = 87.5 G .

For the static load condition, the bolt would be elongated 0.00218 inches. For the impact case, it was assumed that the effective force acting at the top of the bolt is equal to half the weight of the bolt plus the weight of the anchor nut. The weight of the bolt is 2.67 lb per ft and the weight of the 4-inch-diameter nut is 42.73 lb per ft. Thus the total effective force is

$$F = (1/2)(2.67)(49.75)(87.5)/12 + (42.73)(3.5)(87.5)/12 = 1575 \text{ lb.}$$

TABLE 2. RESULTS OF ANALYSIS OF TOP END IMPACT ORIENTATION

Load Condition	At Point A[a] Stress, psi		Deflection relative to Point C, inches	At Point B[a] Stress, psi		At Point C[a] Stress, psi	
	Inner Surface	Outer Surface		Inner Surface	Outer Surface	Inner Surface	Outer Surface
Static 1000 lb	5,412	-5,492	-0.00433	-5,333	4,862	472	- 943
Inertia of can bottom & can walls only, no restraint from bolt	3,624	-3,715	-0.00607	-6,299	5,317	3,608	-7,217
Total	8,036	-9,207	-0.01040	-11,632	10,179	4,080	-8,160

(a) Refer to Figure 2.

Therefore, the total compressive deformation is 0.00344 inches. The effect of the inertia loading on the bolt itself would be to relieve the tensile load on the bolt and place it in a compression. Its total deflection then is 0.00344 + 0.00218 = 0.00563 inches. Since the bolt would only deflect 0.00562 inches and the bottom, if unsupported, would deform 0.01040 inches, the bolt will provide a significant degree of restraint to deformation of the can. Thus the greatest stress which the can will experience is probably 1/2 to 1/3 the maximum stress of 11,632 psi shown in Table 2. The margin of safety, based on a 30,000 psi yield strength, will be greater than 1.5,

$$(MS = \frac{30,000}{11,632} - 1 = 1.58) \quad .$$

The can also acts as a column under compressive loading. By inspection, it is seen that the case for the bottom end impact is more severe than for the top end impact since the impact force, 368 G, is greater and the cover is heavier than the can bottom. Thus, the column action of the can was not evaluated here.

Analyses of the effect of the added load from the can on the draw bolt was not considered necessary. The bolt closely fits through cover and thus misalignment during impact is prevented. Should the bolt experience any plastic deformation during the impact, it would not be detrimental to the seal. Any "shortening" of the bolt due to the impact would produce a greater tensile load in the bolt tending to keep the cover in place. Therefore, the above analyses have indicated that the integrity of the can and seal are maintained during a top end impact condition.

2. Bottom End Impact

In the event of an impact on the bottom end, the inertia force of the cover will tend to increase the pressure on the seal at the edge of the cover. However, the pressure on the seal under the head of the draw bolt could be lessened. The possibility of this occurring is evaluated below. The MONSA computer program was used to evaluate the model shown in Figure 3a for the static condition and for the inertia effect on the cover as if the

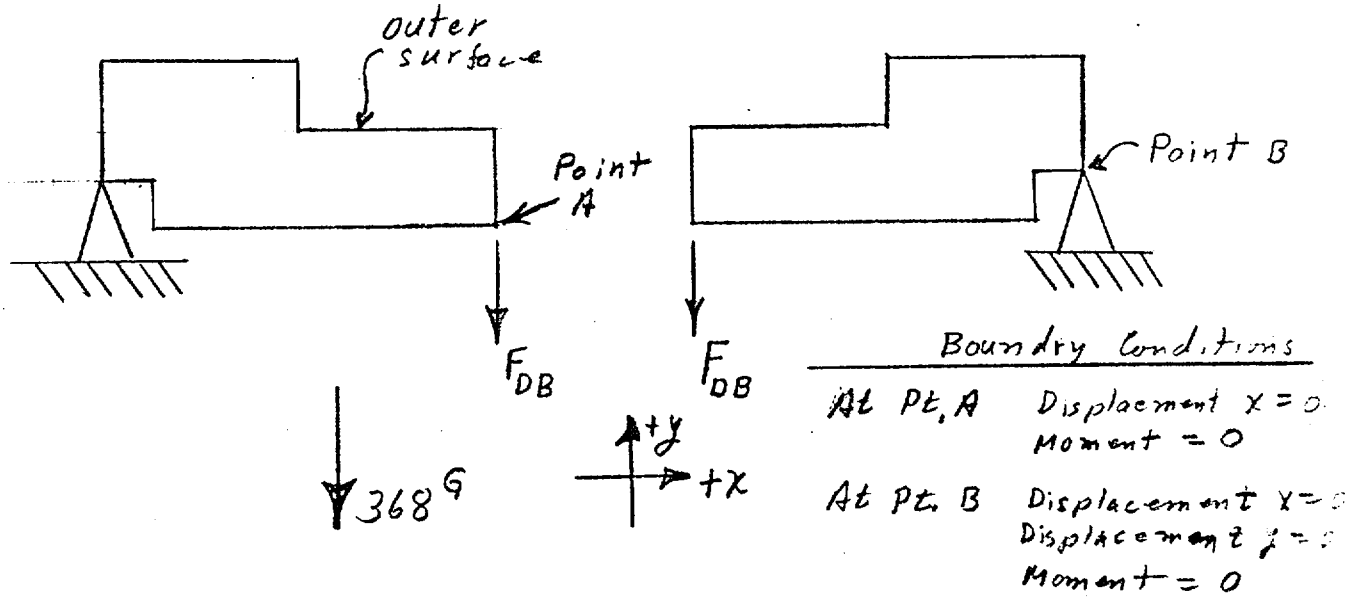

a) Cover

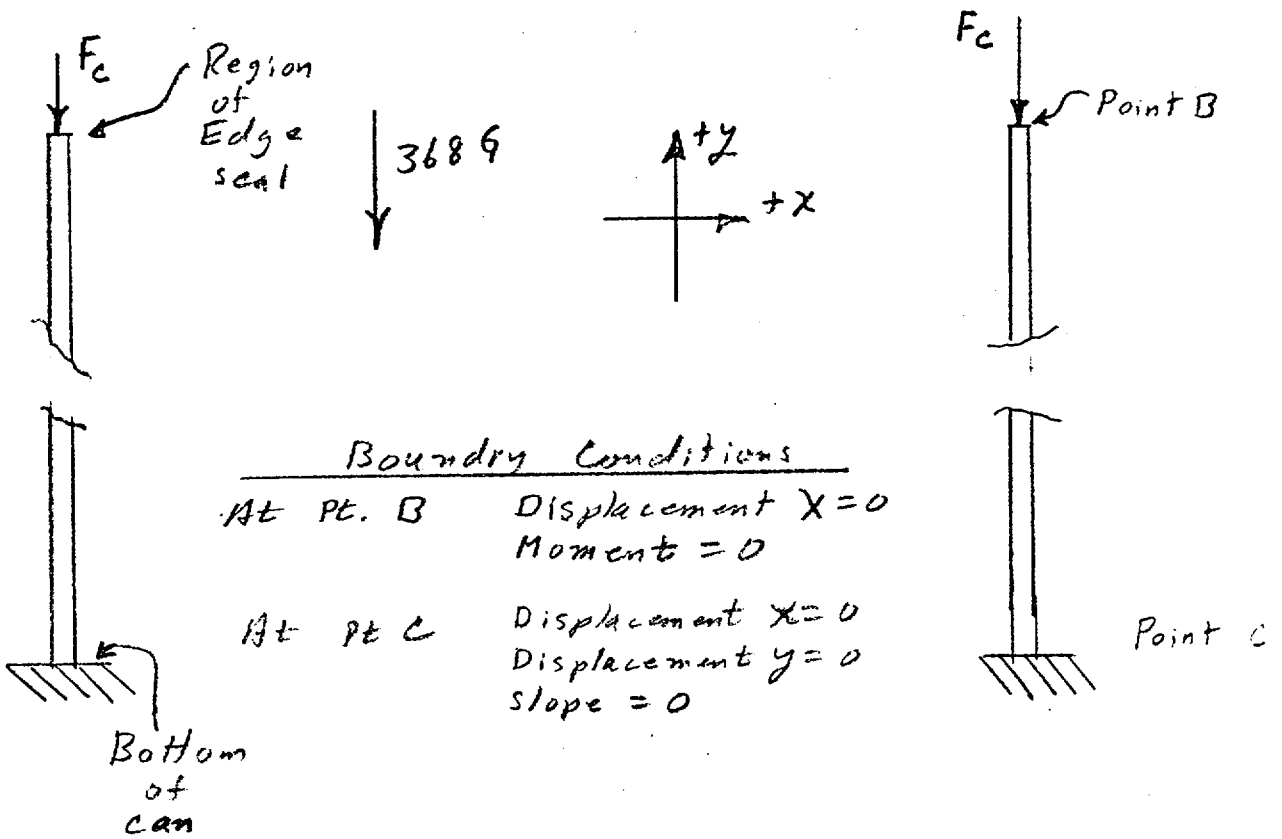

b) Shell

FIGURE 3. ANALYTICAL MODEL FOR BOTTOM END IMPACT ORIENTATION

draw bolt were not present. The maximum deflection of the cover, Point A in Figure 3a, relative to the outer seal, Point B, was calculated to be 0.00340 inches under the combined static and inertia load, Table 3. The MONSA program was then used to analyze the model of the can shell alone, shown in Figure 3b. The force F_c is 1000 lb for the static case and, for the impact case, F_c is the total inertia force of the cover acting on the top edge of the can. The cover weighs 65.67 lbs. Thus for the 368 G inertia load the force, F_c, is 24,170 lb. The total deflection of the shell alone under the static load is 0.00042 inches. Under the inertia load of the cover and the shell, the deflection is 0.01507 inches (Point B to Point C in Figure 3b). Thus, the total deflection of the shell only is 0.01549 inches, and the total deflection of the cover, Point A, relative to the bottom of the can, Point C, is 0.01889 inches.

It was shown above that the bolt is elongated 0.00218 inches under the static 1000 lb load. It was also shown above that the bolt will compress axially 0.00344 inches under a 87.5 G load. Thus, under a 368 G load the bolt will compress (368)(0.00344)/87.5 or 0.01466 inches. Thus the total deflection which the bolt will experience is 0.00218 + 0.01446 = 0.01664 inches. Since this is less than the deflection of the cover, the bolt does not contribute any load to the cover under the impact condition. These calculations indicate that the compression on the seal under the bolt head will be relieved 0.00225 inches. However, the seal is initially compressed about 0.030 inches so that this amount of relief under impact represents only about 7.5 percent of the initial amount. Stated another way, the O-ring is still compressed over 90 percent of its initial amount which is considered sufficient to maintain the seal.

The maximum stress in the can, Table 3, is 17,667 psi. The margin of safety is

$$MS = \frac{30,000}{17,667} - 1 - 0.70.$$

The can also acts as a column under a compressive load equal to the inertia weight of the cover and can shell. It was assumed that the total inertia load experienced by the can as a column is equivalent to the cover weight and half of the inertia "weight" of the shell. From above, the inertia

TABLE 3. RESULTS OF ANALYSIS OF BOTTOM END IMPACT

Load Condition	At Point A[a]			At Point B[a]			At Point C[a]	
	Stress, psi		Deflection relative to Point B, inches	Stress, psi		Deflection relative to Point C, inches	Stress, psi	
	Inner Surface	Outer Surface		Inner Surface	Outer Surface		Inner Surface	Outer Surface
Static load on cover only	- 423	-1,689	- 0.00044	145	36	-	-	-
Inertia load on cover only	1,391	-2,787	- 0.00296	1,493	373	-	-	-
Total, static and Inertia of cover on cover only	968	-4,476	- 0.00340	1,638	409	-	-	-
Static load on shell only	-	-	-	- 236	-236	- 0.00042	- 107	- 364
Inertia Load of shell & cover on shell only	-	-	-	-5,696	-5,696	- 0.01507	-5,146	-17,293
Total, static and Inertia of cover & shell on shell only	-	-	-	-5,932	-5,932	- 0.01549	-5,253	-17,667

(a) Refer to Figure 3.

weight of the cover is 24,170 lb. The static weight of the shell is 63.27 lb. Thus, total inertia load on the can shell as a column is

$$P = 24,170 + (1/2)(368)(63.27) = 35,810 \text{ lb.}$$

The critical buckling load for a column rigidly fixed at one end is

$$P_{crit} = \pi^2 EI/4L^2 \quad ,$$

where

E = Youngs Modulus = $29(10^6)$ psi

I = Moment of inertia = $\pi d^3 t/8$

d = Mean diameter = 14.91 inches

t = Thickness = 0.09 inches

L = Length = 51.75 inches.

Then

$$P_{crit} = 3.13(10^6) \text{ lb} \ .$$

Thus, the can will not buckle.

As above, any deformation or shortening of the draw bolt due to the impact incident would not be detrimental to the integrity of the seal. Therefore, it was not considered necessary to evaluate the impact effect on the bolt.

3. Corner Drop

The fuel can fits in the cask cavity with only nominal clearance. Thus for the corner drop orientation the can is supported both on the side and an end. Since the impact loads for the corner drop orientation are less severe (153 G) than for the impact loads for the bottom end drop or side drop configurations, the analyses for the bottom corner drop configuration need not be evaluated. For the case of a top corner impact orientation, the 153 G impact force is greater than that experienced by the cask for the top end drop configuration, 87.5 G. However, the aspect ratio of the cask (L/d) is relatively large; thus the top edge drop orientation is very close to the vertical orientation of the end fall condition. The response of the fuel can to a top corner impact orientation can then be evaluated by taking the conservative approach and assume it strikes on the top end with the 153 G impact force. This is conservative since for the end impact orientation, no support is considered by the side walls of the cask cavity.

The response of the fuel can is proportional to the impact load. Since for the assumed case here the impact force is 153 G, the stresses and deflections experienced by the fuel can would be 153/87.5 = 1.75 times greater than for the case of the top end drop orientation. By inspection, it is seen that the stresses are well below the yield stress and thus the can integrity is maintained. Similarly, by inspection it is seen that the seals will not be loosened for the top corner impact orientation and thus seal integrity is maintained.

4. Side Impact

For the side impact orientation, the side of the can and the cover are supported by the full length of the cask cavity. Thus the critical regions which must be considered include the stress and deflection in several regions of the draw bolt and the integrity of the seal under loads and moments transmitted by the bolt. A general schematic model of the can is shown in Figure 4. As shown, the bolt is rigidly supported at the bottom by the anchor nut and at the top by the close fitting hole in the cover. It also nominally has a center support, the spacer can bottom, except that the spacer can has a 0.090 inch radial clearance and thus the center of the bolt could deflect about 0.095 inches (the spacer can guide clearance plus the bolt clearance) before any degree of support could be expected.

Consider the model in Figure 5. The bolt is represented as a beam under a tensile load, restrained at the ends from bending and with a center support available after 0.095 inch of deflection. In the actual situation the "center" support is about 1.38 inches from the midlength of the bolt. For purposes of analysis it was considered sufficiently accurate to assume that deflections at the center and 1.38 inches from the center were essentially the same. Then from Roach[1], Table VI, Case 18, the deflection at the center is

$$y = \frac{wj^2}{8p}\left[\frac{4\,U(1 - \cosh U/2)}{\sinh U/2} + U^2\right] \quad ,$$

(1) Roach, R. J., Formulas for Stress and Strain, 4th Edition, McGraw Hill Book Co., New York.

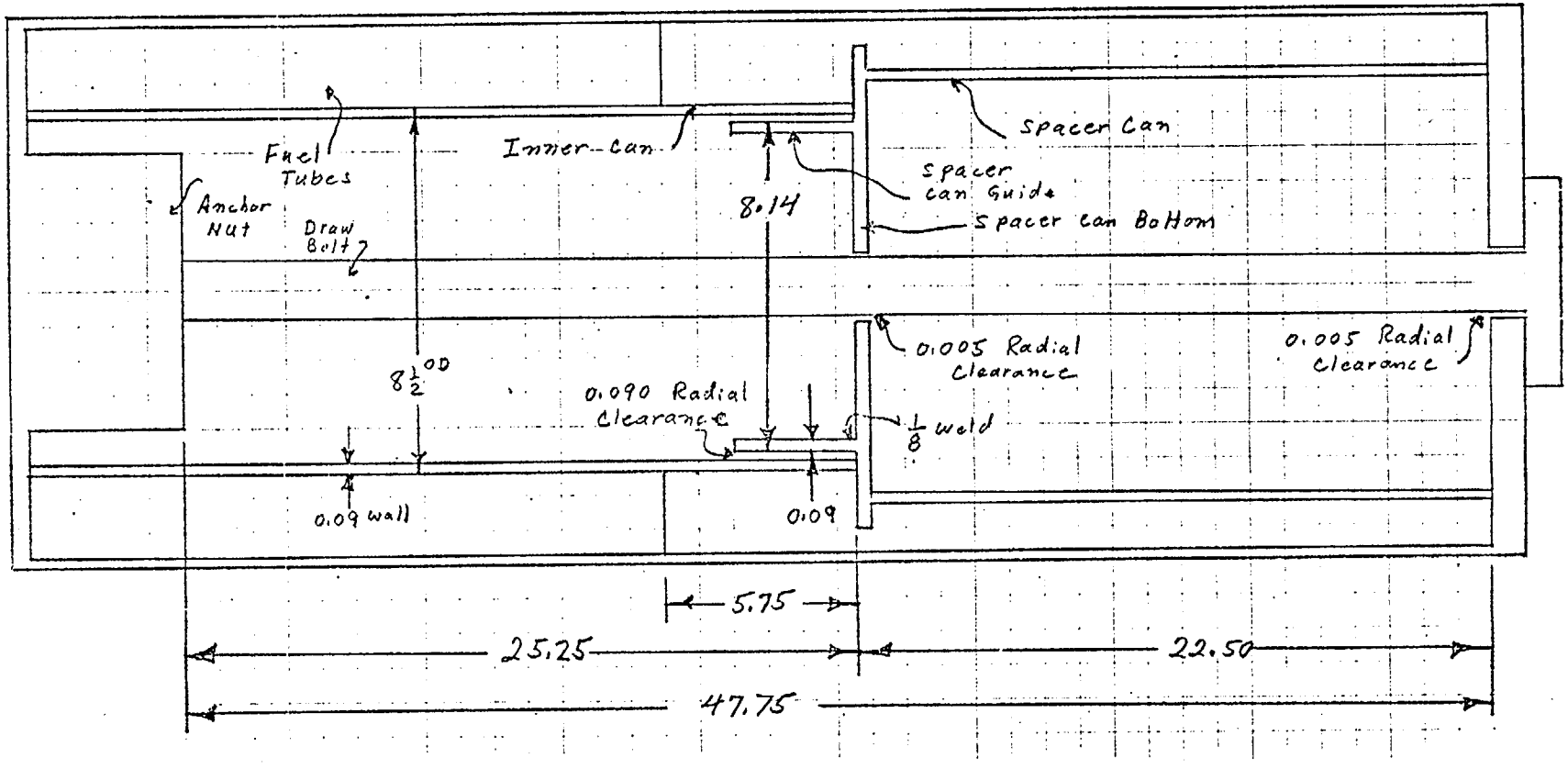

FIGURE 4. SCHEMATIC OF FUEL CAN FOR SIDE IMPACT ORIENTATION

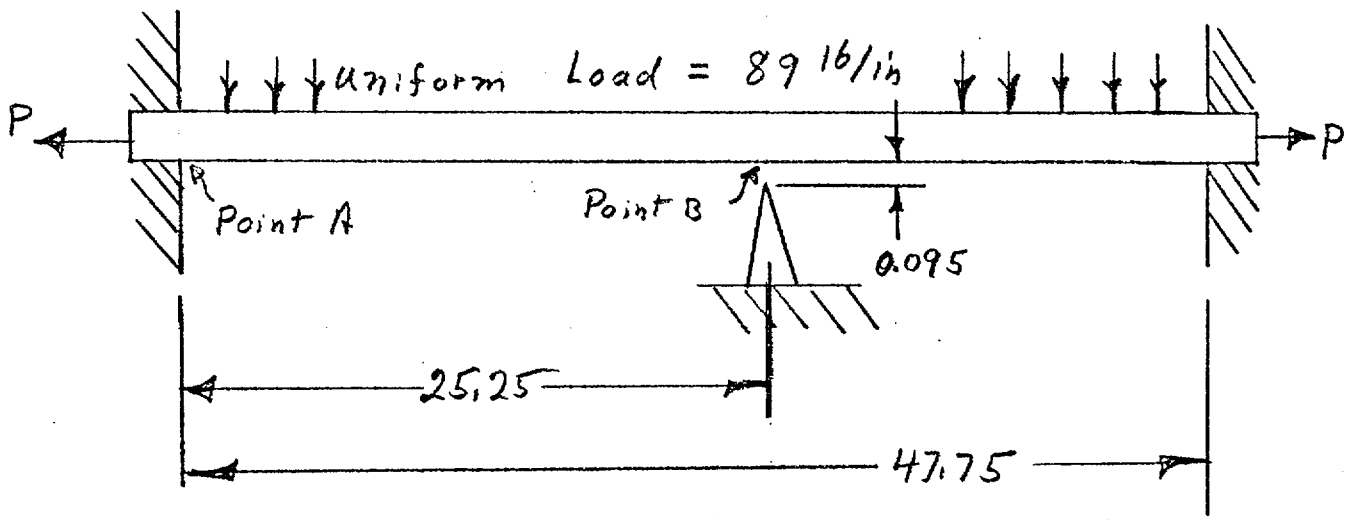

FIGURE 5. MODEL OF DRAW BOLT FOR SIDE IMPACT ORIENTATION

where

w = uniform load

$j = \sqrt{\frac{EI}{P}}$

E = Elastic modulus = $29(10^6)$ psi

I = Area moment of inertia = $\pi(D_o^4 - D_i^4)/64$

D_o = OD of draw bolt = 1.25 inches

D_i = ID of draw bolt = 0.75 inch

P = Tensile load = 1000 lb

$U = L/j$

L = Length of the bolt = 47.75 inches.

This equation was solved for w for the case where y = 0.095. At this deflection w = 21.62 lb per inch. However, the bolt weighs 2.67 lb per ft and, therefore, under a 400 G impact force the distributed load would be 89.0 lb per inch. Since this is more than the 21.62 lb per inch distributed load required to deflect the center of the bolt 0.095 inch, the bolt will receive support from the spacer can bottom under the 400 G impact. The maximum moment in the bolt occurs at the end and is expressed as

$$M = wj^2 \left[(U/2)/ \tanh U/2 - 1 \right] .$$

With a distributed load of 21.62 lb per inch, the moment is 4,058 in lb.

After the bolt receives support from the spacer can bottom it then, for practical purposes, will respond as before, a beam with fixed ends and under a tension load. This is not truely the case since the "center" support is not truely at the midspan but 1.38 inches away. However, it is felt that negligible error will be introduced by this assumption. The calculation is as above, then, except that w = 89.0 lb per inch and L = 25.25 inches.

Then

$$M = 4{,}712 \text{ in. lb.}$$

This is greater than the moment experienced by the bolt at the point it obtained support from the spacer can bottom. The fiber stress then is

$$\sigma = \frac{MC}{I} ,$$

where

M = 4,712 in lb

C = Maximum fiber distance from neutral axis of 1-inch bolt in end of draw bolt (at thread root) = 0.4517 inches.

I = Moment of inertia of 1-inch bolt at thread root = $\pi C^4/4$.

Then the fiber stress is

$$\sigma_f = 65,100 \text{ psi} .$$

The shear stress is

$$\sigma_{sh} = \frac{F_{sh}}{A} .$$

The shear force, F_{sh}, was taken as half the impact force or

$$F_{sh} = wL/2 = (89.0)925.25)/2 = 1125 \text{ lb} .$$

The shear area, A, is

$$\pi c^2 = (\pi)(0.4517)^2 = 0.641 \text{ sq inch} .$$

The shear stress is

$$\sigma_{sh} = 1125/0.641 = 1,760 \text{ psi} .$$

The combined stress is

$$\sigma_{comb} = \sqrt{\sigma_f^{\,2} + \sigma_{sh}^{\,2}} \cong 65,100 \text{ psi} .$$

The threaded section of the bolt is made of A 325 steel which has a yield strength of 92,000 psi. The margin of safety is

$$MS = \frac{F_y}{\sigma_{comb}} - 1 = \frac{92,000}{65,100} - 1 = 0.41 .$$

At the center of the span the bending moment is

$$M = wj^2 \left(1 - \frac{U/2}{\sinh U/2}\right)$$

where the terms are defined as above and w = 89.0 lb per inch and L = 25.25 inches.

Then

$$M = 2350 \text{ inch-lb} .$$

The stress is

$$\sigma_f = Mc/I ,$$

where

M = 2350 in-lb

c = Maximum fiber distance = 1.25/2 = 0.625 inch

I = Moment of inertia = $\pi(D_o^{\,4} - D_i^{\,4})/64$

D_o = 1.25 inches

D_i = 0.75 inch .

Then

$$\sigma_f = 12,260 \text{ psi} .$$

The body of the bolt is made of C-1018 cold rolled carbon steel which has a yield strength of 60,000 psi. The margin of safety is

$$MS = \frac{60,000}{12,260} - 1 = 3.89 .$$

The above analyses assume that the center support, i.e., the spacer can bottom will not move radially more than about 0.095 inch. The spacer can is supported by the guide tube which fits into the inner can. The inner can is rigidly held by the nest of fuel tubes except for the end most 5.75 inches into which the spacer can guide fits. This 5.75 inch extension, therefore, acts as a cantilever beam in supporting the spacer can bottom. Consider the model of Figure 6. The fiber stress in the inner can is

$$\sigma = \frac{MC}{I} = \frac{FLc}{I} ,$$

where

F = Inertia force of bolt and spacer can

L = Length of inner can extension = 5.75 inches

c = Maximum fiber distance = 4.25 inches

I = Moment of inertia = $\pi d^3 t/8$

d = Mean diameter = 8.41 inches

t = Thickness = 0.09 inch .

The force was taken as half the inertia weight of the bolt and 3/4 the inertia weight of the spacer can. The spacer can has a static weight of about 35 lb. Then the inertia force is

$$F = (89.0)47.75)/2 + (400)(35)(3/4) = 12,620 \text{ lb} .$$

Then

$$\sigma_f = 14,680 \text{ psi} .$$

The shear stress is

$$\sigma_{sh} = F/A = 12,620/(\pi dt) = 5,300 \text{ psi.}$$

The combined stress is

$$\sigma_{comb} = \sqrt{\sigma_f^2 + \sigma_{sh}^2} = 15,600 \text{ psi.}$$

The margin of safety for the inner can which is made of Type 304 stainless steel is

$$MS = \frac{Fy}{\sigma_{comb}} - 1 = \frac{30,000}{15,600} - 1 = 0.92 .$$

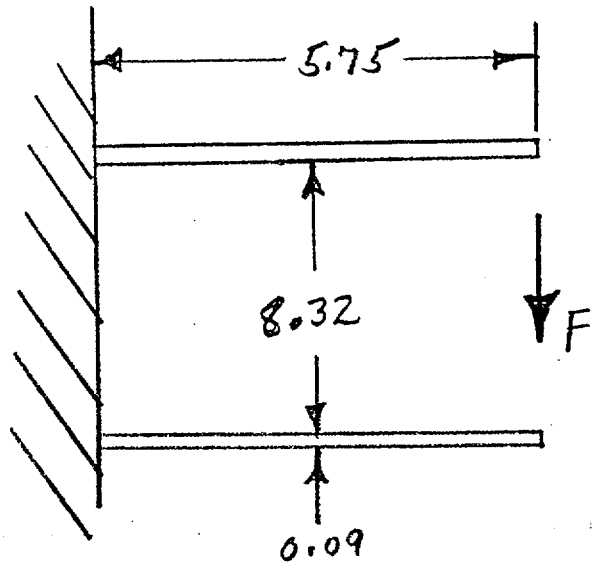

FIGURE 6. MODEL OF INNER CAN

The total deflection is

$$y = FL^3/3EI = 0.0013 \text{ inch.}$$

Thus, the spacer can will move 0.0013 inch more than the 0.095 inch assumed above. This difference, however, will not significantly change the results presented above.

The integrity of the weld between the spacer can guide and the spacer can bottom must also be evaluated. The stress is

$$\sigma_{sh} = F/A = 12{,}620/(0.707\ \pi dt)\ ,$$

where

$$d = \text{Mean weld diameter} \cong 7.90 \text{ inches}$$

$$t = \text{Weld thickness} = 0.12 \text{ inch.}$$

Then

$$\sigma_{sh} = 5{,}990 \text{ psi}\ .$$

The margin of safety is

$$MS = \frac{F_{sh}}{\sigma_{sh}} - 1 = \frac{15{,}000}{5{,}990} - 1 = 1.50\ .$$

In the side fall incident, the bending moment present in the bolt at the cover will tend to "lift" one edge of the seal. The close fit of the bolt in the cover negates any possibility of "lifting" of the seal under the bolt head. However, the tendency for lifting of the seal at the edge of the cover must be evaluated. Consider the model in Figure 7. The moment, M, tends to lift the seal at Point B while the moment of the draw bolt tensile force, P, about Point A tends to maintain the seal at Point B. The moment, M, is assumed to be the same as the moment in the draw bolt at the anchor nut. (It actually will be slightly less since the unsupported span of the top part of the bolt is 2.75 inches shorter than the bottom part.) Then, M = 4,712 in lb. The restoring moment is

$$M_R = Pd/2 = (1000)(15/2) = 7500 \text{ in-lb}\ .$$

This is about 60 percent greater than the moment tending to open the seal. Thus the tendency for lifting is sufficiently restrained to maintain the seal.

The conclusion of the above analysis is that the integrity of the fuel can and seal is maintained in the event of a side fall impact orientation.

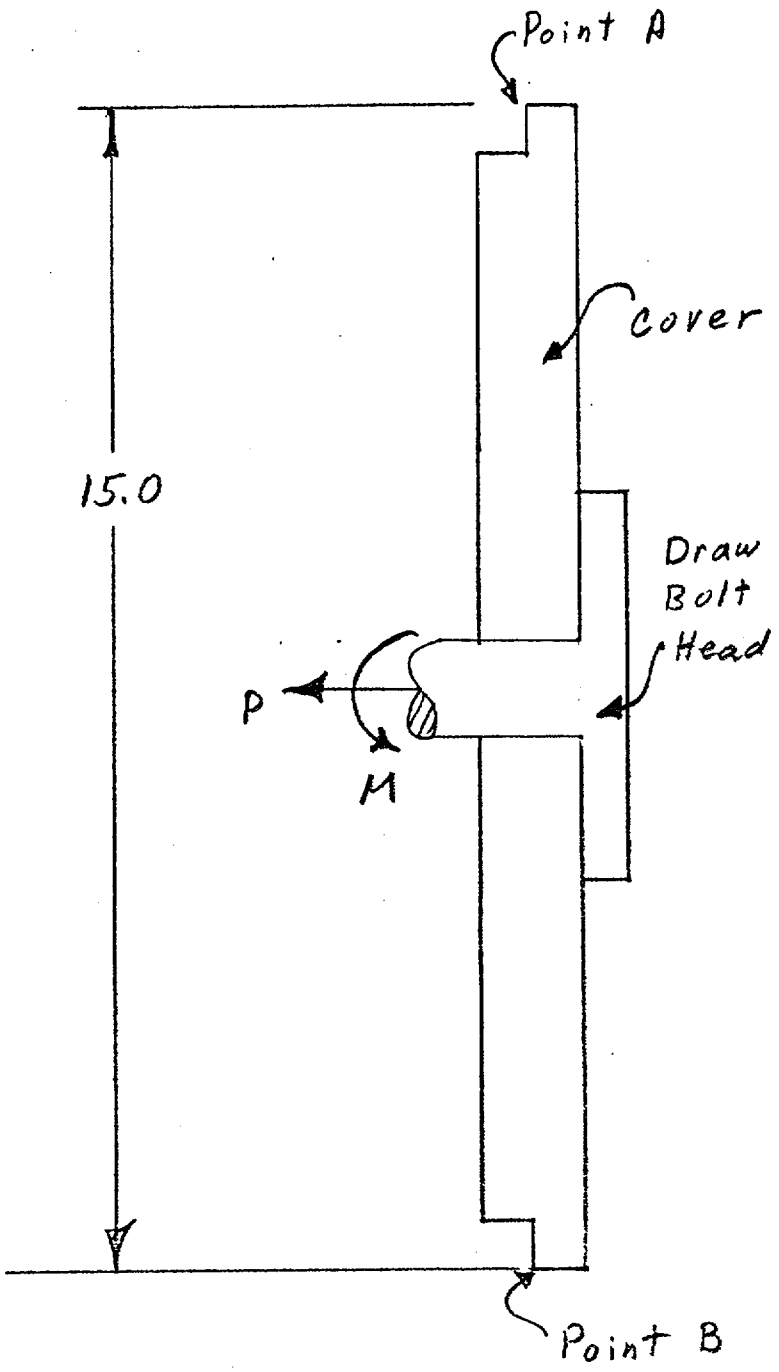

FIGURE 7. MODEL OF FUEL CAN COVER FOR SIDE IMPACT ORIENTATION

5. O-Ring Material

All applicable drawings and operation procedures have been revised to reflect the use of only silicone rubber (silastic) seal materials.

6. Thread Sealant

There are no plugs on fuel can which form part of the sealing system. The operating procedures for the shipping cask specify the use of a non-hardening thread sealant.

7. Basis of Criticality Analysis

Appendix B contains an extract from proprietary Report GAMB-7445 which forms the basis of the criticality analyses.

APPENDIX A

DESCRIPTION OF MONSA COMPUTER PROGRAM

APPENDIX A

DESCRIPTION OF MONSA COMPUTER PROGRAM

MONSA (multilayer Orthotropic Nonsymmetric Shell Analysis) is a digital computer program written in FORTRAN IV. It is based on the multi-segment numerical integration method for the analysis of boundary value problems.

MONSAS determines the displacements, forces, and stresses for a composite shell of revolution. A composite shell is defined as a shell composed of a number of distinct parts which may have the following shapes: cylindrical, spheroidal, ellipsoidal, paraboloidal, conical and toroidal. The shell wall may be composed of four different layers of orthotropic materials. The shell layers are specified by giving their location with respect to a reference surface.

Mechanical and temperature loadings can be applied to the shell. For nonsymmetric loadings, the user must determine the Fourier harmonics of the loadings and perform the appropriate number of shell calculations. Temperatures can vary along the shell meridian as well as through the thickness of the wall. The latter can be accomplished by specifying the temperature on the inner and outer surfaces and on three internal surfaces of the shell wall. A shell spinning about its longitudinal axis can be analyzed. A shell subjected to harmonically varying mechanical or temperature loadings can also be analyzed.

MONSAV will determine the natural frequencies and mode shapes of composite shells of revolution described above. The procedure is based on an iterative technique in which a trial frequency is picked and a determinant is calculated. The trial frequency becomes a natural frequency when the determinant vanishes.

Sept. 1964

Analysis of Shells of Revolution Subjected to Symmetrical and Nonsymmetrical Loads[1]

A. KALNINS

Assistant Professor
of Engineering and Applied Science,
Yale University,
New Haven, Conn.
Mem. ASME

The boundary-value problem of deformation of a rotationally symmetric shell is stated in terms of a new system of first-order ordinary differential equations which can be derived for any consistent linear bending theory of shells. The dependent variables contained in this system of equations are those quantities which appear in the natural boundary conditions on a rotationally symmetric edge of a shell of revolution. A numerical method of solution which combines the advantages of both the direct integration and the finite-difference approach is developed for the analysis of rotationally symmetric shells. This method eliminates the loss of accuracy encountered in the usual application of the direct integration approach to the analysis of shells. For the purpose of illustration, stresses and displacements of a pressurized torus are calculated and detailed numerical results are presented.

The shell of revolution is an important structural element, and the literature devoted to its analysis is extensive. With regard to axisymmetric deformation, various methods have been employed to obtain solutions of the bending theory of shells of revolution by means of the H. Reissner-Meissner equations. For example, Naghdi and DeSilva [1][2] use asymptotic integration; Lohmann [2], Münz [3], Klingbeil [4], employ a direct numerical integration approach; Galletly, et al. [5] find the solution for an ellipsoidal shell of revolution by both the finite-difference and the Runge-Kutta method; and Penny [6], Radkowski, et al. [7], and Sepetoski, et al. [8] utilize the finite-difference technique. A number of additional references which deal with the solution of the H. Reissner-Meissner equations can be found in the papers cited.

For problems of bending in the absence of axial symmetry, a reduction of the governing equations of arbitrary shells of revolution to a system of four second-order differential equations involving four unknowns has been carried out by Budiansky and Radkowski [9]. A method for obtaining the solution of these equations is given in [9] which is an extension of that employed in [7] and [8]. Furthermore, treatments of nonsymmetric deformation of shells of revolution are found in papers by Goldberg and Bogdanoff [10], where a system of first-order differential equations for conical shells is derived, and by Steele [11] and Schile [12], where solutions of certain types are considered by means of asymptotic integration.

Among the papers which employ numerical analysis, two dif-

[1] National Science Foundation Grant No. 23922, Report No. 3, July, 1963.

[2] Numbers in brackets designate References at end of paper.

Presented at the Summer Conference of the Applied Mechanics Division, Boulder, Colo., June 9–11, 1964, of The American Society of Mechanical Engineers.

Discussion of this paper should be addressed to the Editorial Department, ASME, United Engineering Center, 345 East 47th Street, New York, N. Y. 10017, and will be accepted until October 10, 1964. Discussion received after the closing date will be returned. Manuscript received by ASME Applied Mechanics Division, July 31, 1963. Paper No. 64—APM-33.

Nomenclature

ϕ, θ, ζ = coordinates of a point of shell

s = distance measured from an arbitrary origin along meridian in positive direction of ϕ

$\mathbf{t}_\phi, \mathbf{t}_\theta, \mathbf{n}$ = unit vectors tangent to coordinate curves (see Fig.

R_ϕ, R_θ = principal radii of curvature of middle surface

r = distance of a point on middle surface from axis of symmetry

E = Young's modulus

ν = Poisson's ratio

h = thickness of shell

α = coefficient of thermal expansion

$D = Eh^3/[12(1-\nu^2)]$

$K = Eh/(1-\nu^2)$

u_ϕ, u_θ, w = components of displacement of middle surface

β_ϕ, β_θ = angle of rotation of normal

p_ϕ, p_θ, p = components of mechanical surface loads

m_ϕ, m_θ = components of moment of surface loads

T, T_0, T_1 = temperature increment and temperature resultants

$N_\phi, N_\theta, N_{\theta\phi}$ = membrane stress resultants

$M_\phi, M_\theta, M_{\theta\phi}$ = moment resultants

Q_ϕ, Q_θ = transverse-shear resultants

$\bar{N}, \bar{Q}$ = effective shear resultants

$J = 1/R_\phi + \sin\phi/r$

$U = 1/R_\phi + r\sin\phi/\Delta$

$R = 1/R_\phi - \sin\phi/r$

n = integer, designating nth Fourier component

β = length factor

$(\ )_{,x}$ = derivative with respect to any coordinate

m = order of system of equations

M = number of segments

x = independent variable, either ϕ or s

x_i = end point of segment

$y(x)$ = $(m, 1)$ matrix, fundamental variables

$A(x)$ = (m, m) matrix, coefficients of differential equations

$B(x)$ = $(m, 1)$ matrix, nonhomogeneous coefficients

$Y(x)$ = (m, m) matrix, homogeneous solution

$Z(x)$ = $(m, 1)$ matrix, particular solution

C = $(m, 1)$ matrix, arbitrary constants

I = unit matrix

ferent methods of solution of the boundary-value problem of deformation of shells must be recognized; i.e., the direct integration [2–5] and the finite difference [illegible] each [5–9]. While the direct integration approach has certain important advantages, it also has a serious disadvantage; i.e., when the length of the shell is increased, a loss of accuracy invariably results. This phenomenon was clearly pointed out in [8]. The loss of accuracy does not result from accumulative errors in integration, but it is caused by the subtraction of almost equal numbers in the process of determination of the unknown boundary values. It follows that for every set of geometric and material parameters of the shell there is a critical length beyond which the solution loses all accuracy. The advantage of the finite-difference approach over direct integration is that it can avoid such a loss of accuracy. It is concluded from [8] that if the solution of the system of algebraic equations, which result from the finite-difference equations, is obtained by means of Gaussian elimination, then no loss of accuracy is experienced if the length of the shell is increased.

This paper is concerned with the general problem of deformation of thin, elastic shells of revolution, symmetrically or nonsymmetrically loaded, and with the development of a numerical method of its solution, which employs the direct integration technique, but eliminates the loss of accuracy owing to the length of the shell. The method developed here is applicable to any two-point boundary-value problem which is governed within an interval by a system of m first-order linear ordinary differential equations together with $m/2$ boundary conditions prescribed at each end of the interval. It is shown that the boundary-value problem of a rotationally symmetric shell can be stated in this form for any consistent linear bending theory of shells in terms of those quantities which appear in the natural boundary conditions on a rotationally symmetric edge.

The method of this paper offers definite advantages over the finite-difference approach. The main advantages are: (*a*) It can be applied conveniently to a large system of first-order differential equations, and (*b*) it permits an automatic selection of an optimum step size of integration at each step according to the desired accuracy of the solution. The first point means that the equations of the theory of shells of revolution, characterized in terms of first-order differential equations, can be integrated directly, and further reduction of the equations to a smaller number of unknowns is not necessary. The second point seems to be of great importance if a truly general method is desired which is expected to hold for arbitrary loads, shell configurations, thickness, and so on. With the finite-difference approach, a meaningful *a priori* estimate of the step size is often difficult, if not impossible, especially when rapid changes and discontinuities in the shell parameters are encountered. If a predictor-corrector direct integration approach is employed with the method of this paper, then the step size can be selected automatically at each step which ensures a prescribed accuracy of the solution and optimum efficiency in the calculation.

The method given in this paper can be divided into two parts: (*a*) Direct integration of $m + 1$ initial value problems over preselected segments of the total interval, and (*b*) the use of Gaussian elimination in the solution of the resulting system of matrix equations. The part of this method is a generalization of that which is [illegible] over the whole interval in [2–5]. Here, however, the initial value problems are defined over segments of the total interval, lengths of which are within the range of the applicability of the direct integration approach. After the initial value problems are integrated over these segments, continuity conditions on the variables are written at the endpoints of the segments, and they constitute a simultaneous system of linear matrix equations. This system of matrix equations is then solved directly by means of Gaussian elimination. The result is that the direct integration method is employed and at the same time there is no loss of accuracy because the lengths of the segments are selected in such a way that the solutions of the initial value problems are kept sufficiently small. A convenient parameter is given from which the appropriate lengths of the segments can be estimated easily.

In the application of this method to the analysis of rotationally symmetric shells, the boundary-value problem is formulated in terms of first-order ordinary differential equations. For this purpose, starting with the equations of the linear classical bending theory of shells in which the thermal effects are included, first a system of equations is derived in the form of eight partial differential equations involving eight unknowns in such a manner that the system of equations contains no derivatives of the material parameters, thickness, or principal radii of curvature. The absence of the derivatives in the coefficients of the differential equations permits the calculation of the coefficients at a point without regard to the values of the shell parameters at preceding or following points. Then, assuming separability with respect to the independent variables, the desired system of eight first-order ordinary differential equations is obtained which together with the boundary conditions on two edges of the shell constitute a two-point boundary-value problem. The derived system of equations is applicable to rotationally symmetric shells with arbitrary meridional variations (including discontinuities) in Young's modulus, Poisson's ratio, radii of curvature, thickness, and coefficient of thermal expansion. While such a system of equations is derived in this paper only for one version of the classical theory of shells, it can be derived in the same way for all other consistent linear bending theories of shells, including those which account for the dynamic effects, transverse shear deformation, nonhomogeneity, and anisotropy.

Finally, with the use of the method and the equations given in this paper, stresses and displacements are calculated in a thin-walled torus subjected to internal pressure. The solution shows that the meridional membrane stress is almost identical to that predicted by membrane theory, but that the bending stresses even for a relatively thin torus may not be negligible.

Geometry and Basic Equations

The position of a point of a shell of revolution is given by the coordinates θ, ϕ, ζ measured along the triplet of unit vectors $\mathbf{t}_\theta$, $\mathbf{t}_\phi$, $\mathbf{n}$, respectively, as shown in Fig. 1. The shape of the shell is determined by specifying the two principal radii of curvature R_ϕ, R_θ of the middle surface as functions of ϕ. Instead of R_θ, it is convenient to use the distance r from a point on the middle surface to the z-axis; from Fig. 1 it follows that

$$r = R_\theta \sin \phi \tag{1}$$

If the generating curve of the middle surface is given by $r = r(z)$ then

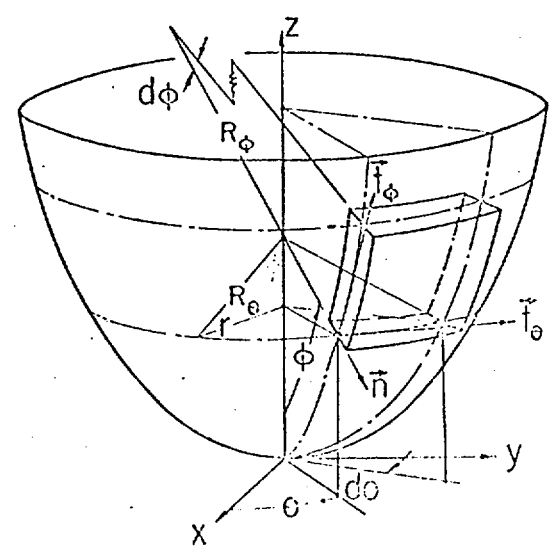

Fig. 1 Element of a shell of revolution

$$R_\phi = -\left[1 + \left(\frac{dr}{dz}\right)^2\right]^{3/2} \Big/ \frac{d^2r}{dz^2}$$

$$R_\theta = r\left[1 + \left(\frac{dr}{dz}\right)^2\right]^{1/2} \tag{2}$$

The following analysis requires frequent differentiation of r (or R_θ) with respect to ϕ, and it is convenient to express this derivative by the Codazzi relation

$$\frac{dr}{d\phi} = R_\phi \cos\phi \tag{3}$$

The displacement components of the middle surface of the shell and the rotations of the normal are defined by the expression of the displacement vector U of the form

$$\mathbf{U} = (u_\phi + \zeta\beta_\phi)\mathbf{t}_\phi + (u_\theta + \zeta\beta_\theta)\mathbf{t}_\theta + w\mathbf{n} \tag{4a}$$

The shell is subjected to the mechanical load vector p, which is measured as force per unit area of the middle surface and written as

$$\mathbf{p} = p_\phi\mathbf{t}_\phi + p_\theta\mathbf{t}_\theta + p\mathbf{n} \tag{4b}$$

and the moment vector m, which is measured as moment per unit area and given by

$$\mathbf{m} = -m_\theta\mathbf{t}_\phi + m_\phi\mathbf{t}_\theta \tag{4c}$$

With reference to Fig. 1, equations (4) serve the purpose for establishing the positive directions of the components of the displacement and mechanical load vectors.

The temperature distribution in the shell caused by some thermal loads is accounted for in the usual manner by means of the integrated temperature effect of the form

$$T_0(\phi, \theta) = \frac{1}{h}\int_{-\frac{h}{2}}^{\frac{h}{2}} T(\phi, \theta, \zeta)d\zeta \tag{5a}$$

$$T_1(\phi, \theta) = \frac{12}{h^3}\int_{-\frac{h}{2}}^{\frac{h}{2}} \zeta T(\phi, \theta, \zeta)d\zeta \tag{5b}$$

The derivation of a new set of equations carried out in the next section is based on a linear classical theory of shells given by Reissner [13]. When referred to arbitrary shells of revolution, the governing system of equations of [13] can be written in the following form. Equations of equilibrium:

$$N_{\theta,\theta} + \frac{r}{R_\phi}N_{\phi\theta,\phi} + 2\cos\phi\, N_{\theta\phi} + Q_\theta \sin\phi + rp_\theta = 0 \tag{6a}$$

$$N_{\theta\phi,\theta} + \frac{r}{R_\phi}N_{\phi,\phi} + (N_\phi - N_\theta)\cos\phi + \frac{r}{R_\phi}Q_\phi + rp_\phi = 0 \tag{6b}$$

$$Q_{\theta,\theta} + \frac{r}{R_\phi}Q_{\phi,\phi} + Q_\phi\cos\phi - N_\theta\sin\phi - \frac{r}{R_\phi}N_\phi + rp = 0 \tag{7}$$

$$M_{\theta,\theta} + \frac{r}{R_\phi}M_{\phi\theta,\phi} + 2\cos\phi\, M_{\theta\phi} - rQ_\theta + rm_\theta = 0 \tag{8a}$$

$$M_{\theta\phi,\theta} + \frac{r}{R_\phi}M_{\phi,\phi} + (M_\phi - M_\theta)\cos\phi - rQ_\phi + rm_\phi = 0 \tag{8b}$$

Stress-strain relations:

$$N_\theta = K(\epsilon_\theta + \nu\epsilon_\phi) - (1 + \nu)\alpha KT_0 \tag{9a}$$

$$N_\phi = K(\epsilon_\phi + \nu\epsilon_\theta) - (1 + \nu)\alpha KT_0 \tag{9b}$$

$$N_{\theta\phi} = N_{\phi\theta} = (1 - \nu)K\epsilon_{\theta\phi} \tag{9c}$$

$$M_\theta = D(\kappa_\theta + \nu\kappa_\phi) - (1 + \nu)\alpha DT_1 \tag{10a}$$

$$M_\phi = D(\kappa_\phi + \nu\kappa_\theta) - (1 + \nu)\alpha DT_1 \tag{10b}$$

$$M_{\theta\phi} = M_{\phi\theta} = (1 - \nu)D\kappa_{\theta\phi} \tag{10c}$$

Strain-displacement relations:

$$\epsilon_\theta = \frac{1}{r}(u_{\theta,\theta} + u_\phi\cos\phi + w\sin\phi) \tag{11a}$$

$$\epsilon_\phi = \frac{1}{R_\phi}(u_{\phi,\phi} + w) \tag{11b}$$

$$2\epsilon_{\theta\phi} = \frac{1}{r}(u_{\phi,\theta} - u_\theta\cos\phi) + \frac{1}{R_\phi}u_{\theta,\phi} \tag{11c}$$

$$\kappa_\theta = \frac{1}{r}(\beta_{\theta,\theta} + \beta_\phi\cos\phi) \tag{12a}$$

$$\kappa_\phi = \frac{1}{R_\phi}\beta_{\phi,\phi} \tag{12b}$$

$$2\kappa_{\theta\phi} = \frac{1}{r}(\beta_{\phi,\theta} - \beta_\theta\cos\phi) + \frac{1}{R_\phi}\beta_{\theta,\phi} \tag{12c}$$

$$\beta_\theta = -\frac{1}{r}w_{,\theta} + \frac{\sin\phi}{r}u_\theta \tag{13a}$$

$$\beta_\phi = -\frac{1}{R_\phi}w_{,\phi} + \frac{1}{R_\phi}u_\phi \tag{13b}$$

The positive directions of the stress resultants in the foregoing equations are the same as the corresponding stresses on the edge of the shell. The definitions of the stress resultants are found in [13].

The order of the system of equations (6)–(13) is eight with respect to ϕ, and consequently it is possible to reduce (6)–(13) to eight first-order differential equations which involve eight unknowns. If the eight unknowns are those quantities which enter into the natural boundary conditions at the edge ϕ = const, then the boundary-value problem of a rotationally symmetric shell can be completely stated in terms of these unknowns. For this reason, the eight differential equations, derived in the following sections, and the eight unknowns are called the fundamental set of equations and the fundamental variables, respectively.

Derivation of Fundamental Set of Equations

According to the classical theory of shells, the quantities which appear in the natural boundary conditions on a rotationally symmetric edge of a shell of revolution include the effective shear resultants N and Q defined by

$$N = N_{\theta\phi} + \frac{\sin\phi}{r}M_{\theta\phi} \tag{14a}$$

$$Q = Q_\phi + \frac{1}{r}M_{\theta\phi,\theta} \tag{14b}$$

Thus, the fundamental variables, which are consistent with the theory of [13], are the four generalized displacements w, u_ϕ, u_θ, and β_ϕ, and the four generalized forces Q, N_ϕ, N, and M_ϕ.

In the derivation of the fundamental equations, it is [illegible] venient to employ the distance s, measured along the [illegible] the shell, rather than the angular coordinate ϕ. However, after the equations are derived, the problem can again be [illegible] formulated in terms of ϕ by means of the relation

$$\frac{1}{R_\phi}\frac{\partial}{\partial\phi} = \frac{\partial}{\partial s}$$

As a preliminary step, it is necessary to express N_θ, M_θ, $M_{\theta\phi}$ in terms of the fundamental variables. From (9a) it follows that

$$N_\theta = \nu N_\phi + K\frac{1-\nu^2}{r}(w\sin\phi + u_{\theta,\theta} + u_\phi\cos\phi) - \alpha K(1-\nu^2)T_0 \quad (15)$$

and from (10a) that

$$M_\theta = \nu M_\phi + D\frac{1-\nu^2}{r}\left(-\frac{1}{r}w_{,\theta\theta} + \frac{\sin\phi}{r}u_{\theta,\theta} + \beta_\phi\cos\phi\right) - \alpha D(1-\nu^2)T_1 \quad (16)$$

Elimination of $u_{\theta,s}$ and $w_{,s}$ from equation (12c) leads to an expression for $M_{\theta\phi}$ in the form

$$M_{\theta\phi} = LD\frac{1-\nu}{2r}\left[2\beta_{\phi,\theta} + \frac{2\cos\phi}{r}w_{,\theta} + Hu_\theta\cos\phi - Ju_{\phi,\theta}\right] + \frac{LD}{K}\frac{\sin\phi}{r}N \quad (17)$$

where

$$L = \frac{1}{1 + \frac{\sin^2\phi}{r^2}\frac{D}{K}}$$

In the derivation of the four equations of the fundamental set which involve the derivatives of the stress resultants with respect to s, the use of (14) is essential. Elimination of Q_θ from (6a) and (8a) by means of (14a) leads to

$$N_{,s} = H\frac{\cos\phi}{r}M_{\theta\phi} - \frac{2\cos\phi}{r}N - \frac{1}{r}N_{\theta,\theta} - \frac{\sin\phi}{r^2}M_{\theta,\theta} - p_\theta - \frac{\sin\phi}{r}m_\theta \quad (18)$$

Similarly, elimination of Q_θ from (7) and (8a) gives

$$Q_{,s} = -\frac{2\cos\phi}{r^2}M_{\theta\phi,\theta} - \frac{\cos\phi}{r}Q + \frac{\sin\phi}{r}N_\theta + \frac{1}{R_\phi}N_\phi - \frac{1}{r^2}M_{\theta,\theta\theta} - p - \frac{1}{r}m_{\theta,\theta} \quad (19)$$

Solving (6b) from $N_{\phi,s}$ there results

$$N_{\phi,s} = -\frac{1}{r}N_{,\theta} + \frac{1}{r}JM_{\theta\phi,\theta} + \frac{\cos\phi}{r}(N_\theta - N_\phi) - \frac{1}{R_\phi}Q - p_\phi \quad (20)$$

and it follows from (8b)

$$M_{\phi,s} = -\frac{2}{r}M_{\theta\phi,\theta} + \frac{\cos\phi}{r}(M_\theta - M_\phi) + Q - m_\phi \quad (21)$$

Wherever necessary, N_θ and Q_ϕ were eliminated with the use of (14).

The fundamental set of equations consists of (18)-(21), where N_θ, M_θ, $M_{\theta\phi}$ can be replaced directly in terms of the fundamental variables by means of (15)-(17), and four additional equations involving the derivatives of w, u_ϕ, u_θ, β_ϕ with respect to s, which are obtained from (13b), (11c), (11b), (12b), respectively. Finally, the system of eight differential equations that governs the deformation of a shell of revolution can be expressed in terms of the eight fundamental variables and written as

$$w_{,s} = \frac{1}{R_\phi}u_\phi - \beta_\phi \quad (22a)$$

$$u_{\phi,s} = -Uw - \frac{\nu\cos\phi}{r}u_\phi - \frac{\nu}{r}u_{\theta,\theta} + \frac{1}{K}N_\phi + \alpha(1+\nu)T_0 \quad (22b)$$

$$u_{\theta,s} = -\frac{LD\sin 2\phi}{Kr^3}w_{,\theta} - \frac{1}{r}\left(1 - \frac{LDJ\sin\phi}{Kr}\right)u_{\phi,\theta} + \frac{\cos\phi}{r}\left(1 - \frac{LDH\sin\phi}{Kr}\right)u_\theta - \frac{2LD\sin\phi}{Kr^2}\beta_{\phi,\theta} + \frac{2}{(1-\nu)K}\left(1 - \frac{LD\sin^2\phi}{Kr^2}\right)N \quad (22c)$$

$$\beta_{\phi,s} = \frac{\nu}{r^2}w_{,\theta\theta} - \frac{\nu\sin\phi}{r^2}u_{\theta,\theta} - \frac{\nu\cos\phi}{r}\beta_\phi + \frac{1}{D}M_\phi + \alpha(1+\nu)T_1 \quad (22d)$$

$$Q_{,s} = \frac{1-\nu}{r^4}\left[D(1+\nu)\frac{\partial^4}{\partial\theta^4} - 2LD\cos^2\phi\frac{\partial^2}{\partial\theta^2} + (1+\nu)Kr^2\sin^2\phi\right]w + (1-\nu)\frac{\cos\phi}{r^2}\left[\frac{1}{r}LDJ\frac{\partial^2}{\partial\theta^2} + (1+\nu)K\sin\phi\right]u_\phi - \frac{1-\nu}{r^2}\left[\frac{1}{r}LDH\cos^2\phi - (1+\nu)K\sin\phi + D(1+\nu)\frac{\sin\phi}{r^2}\frac{\partial^2}{\partial\theta^2}\right]u_{\theta,\theta}$$
$$- D(1-\nu)\frac{\cos\phi}{r^3}(1+\nu+2L)\beta_{\phi,\theta\theta} + UN_\phi - \frac{\nu}{r^2}M_{\phi,\theta\theta} - \frac{LD\sin 2\phi}{Kr^3}N_{,\theta} - \frac{\cos\phi}{r}Q - p - \frac{1}{r}m_{\theta,\theta} - \alpha(1-\nu^2)\frac{1}{r}\left(K\sin\phi\,T_0 - \frac{1}{r}DT_{1,\theta\theta}\right) \quad (22e)$$

$$N_{\phi,s} = (1-\nu)\frac{\cos\phi}{r^2}\left[\frac{1}{r}LDJ\frac{\partial^2}{\partial\theta^2} + (1+\nu)K\sin\phi\right]w + \frac{1-\nu}{r^2}\left[(1+\nu)K\cos^2\phi - \tfrac{1}{2}LDJ^2\frac{\partial^2}{\partial\theta^2}\right]u_\phi + (1-\nu)\frac{\cos\phi}{r^2}\left[\tfrac{1}{2}LDJH + (1+\nu)K\right]u_{\theta,\theta} + JLD\frac{1-\nu}{r^2}\beta_{\phi,\theta\theta}$$
$$- \frac{1}{R_\phi}Q - (1-\nu)\frac{\cos\phi}{r}N_\phi - \frac{1}{r}\left(1 - \frac{LDJ\sin\phi}{Kr}\right)N_{,\theta} - p_\phi - \alpha(1-\nu^2)K\frac{\cos\phi}{r}T_0 \quad (22f)$$

$$N_{,s} = \frac{1-\nu}{r^2}\left[HLD\frac{\cos^2\phi}{r} - (1+\nu)K\sin\phi + (1+\nu)D\frac{\sin\phi}{r^2}\frac{\partial^2}{\partial\theta^2}\right]w_{,\theta} - (1-\nu)\frac{\cos\phi}{r^2}\left[\tfrac{1}{2}LDJH + (1+\nu)K\right]u_{\phi,\theta}$$
$$+ \frac{1-\nu}{r^2}\left[\tfrac{1}{2}LDH^2\cos^2\phi - (1+\nu)\left(K + \frac{D\sin^2\phi}{r^2}\right)\frac{\partial^2}{\partial\theta^2}\right]u_\theta - D(1-\nu)\frac{\cos\phi}{r^2}\left[(1+\nu)\frac{\sin\phi}{r} - LH\right]\beta_{\phi,\theta} - \frac{\nu}{r}N_{\phi,\theta}$$

$$- \frac{\cos\phi}{r}\left(2 - \frac{LDH\sin\phi}{Kr}\right) N - \frac{\nu\sin\phi}{r^2} \ldots_{,\theta} - p_\theta - \frac{\sin\phi}{r} m_\theta$$

$$+ \alpha(1-\nu^2)\frac{1}{r}\left(KT_{0,\theta} + D\frac{\sin\phi}{r} T_{1,\theta}\right) \quad (22g)$$

$$M_{\phi,s} = -(1-\nu)D\frac{\cos\phi}{r^3}(1+\nu+2L)w_{,\theta\theta} + LDJ\frac{1-\nu}{r^2} u_{\phi,\theta\theta}$$

$$+ D(1-\nu)\frac{\cos\phi}{r^2}\left[(1+\nu)\frac{\sin\phi}{r} - HL\right] u_{\theta,\theta}$$

$$+ D\frac{1-\nu}{r^2}\left[(1+\nu)\cos^2\phi - 2L\frac{\partial^2}{\partial\theta^2}\right]\beta_\phi + Q - \frac{2LD\sin\phi}{Kr^2} N_{,\theta}$$

$$- (1-\nu)\frac{\cos\phi}{r} M_\phi - m_\phi - \alpha(1-\nu^2)D\frac{\cos\phi}{r} T_1 \quad (22h)$$

Equations (22), (14), and (15) to (17) determine all unknown variables except Q_θ which can be found from (8a) and written in the form

$$Q_\theta = \frac{1}{r} M_{\theta,\theta} + M_{\theta\phi,s} + \frac{2\cos\phi}{r} M_{\theta\phi} + m_\theta \quad (23)$$

By calculating $M_{\theta\phi,s}$ from (17) and making use of (16), it is possible to express Q_θ directly in terms of the fundamental variables. This expression is lengthy and contains derivatives with respect to s of the shell parameters. Since Q_θ does not enter into any boundary conditions on the edge s = const, it is preferable to calculate Q_θ as the last unknown directly from (23). The derivative of $M_{\theta\phi}$ can be easily obtained by numerical differentiation.

The procedure for the derivation of an equivalent set of equations for other linear classical theories of isotropic shells is identical to that given before. For general anisotropic and/or nonhomogeneous shells of revolution with rotationally symmetric properties, the fundamental set of equations is derived in the same way as (22) except that (9) and (10) must be replaced by the appropriate stress-strain relations given, for example, by Ambartsumyan [14]. Otherwise, the derivation is straightforward. For the improved theory of shells, such as the one given by Naghdi [15], in which the effects of transverse-shear deformation are accounted for, the following ten fundamental variables are required: $w, u_\phi, u_\theta, \beta_\phi, \beta_\theta, Q_\phi, N_\phi, N_{\phi\theta}, M_\phi, M_{\phi\theta}$. Since now Q_ϕ and Q_θ appear in (13), the elimination of Q_θ from (6a), (8a), is done by means of (13a). The required equations for the derivatives of the generalized forces are obtained directly from the five equations of equilibrium (6), (7), (8). The remaining equations are derived by following a procedure similar to the foregoing.

Fundamental Equations for Separable Solutions

For shells of revolution which consist of complete circles, the surface loads are periodic with respect to period of 2π, and they can be assumed to be of the form

$$\{p_\phi, p_\theta, m_\phi\} = \{p_{\phi n}, p_{\theta n}, m_{\phi n}\}\begin{Bmatrix}\cos n\theta\\ \sin n\theta\end{Bmatrix} \quad (24a)$$

$$\{T_0, T_1\} = \{T_{0n}, T_{1n}\}\begin{Bmatrix}\cos n\theta\\ \sin n\theta\end{Bmatrix} \quad (24b)$$

$$\{p_\theta, m_\theta\} = \{p_{\theta n}, m_{\theta n}\}\begin{Bmatrix}\sin n\theta\\ \cos n\theta\end{Bmatrix} \quad (24c)$$

where the variables with subscripts n depend only on each integral value of n in (24) can be regarded as one component in a general Fourier series expansion of arbitrary periodic surface loads.

Separable solutions of (6)–(8) corresponding to the value of n in (24), are then obtained in the form

$$\{w, u_\phi, \beta_\phi\} = \{w_n, u_{\phi n}, \beta_{\phi n}\}\begin{Bmatrix}\cos n\theta\\ \sin n\theta\end{Bmatrix} \quad (25a)$$

$$\{N_\phi, M_\phi, Q\} = \{N_{\phi n}, M_{\phi n}, Q_n\}\begin{Bmatrix}\cos n\theta\\ \sin n\theta\end{Bmatrix} \quad (25b)$$

$$\{u_\theta, N\} = \{u_{\theta n}, N_n\}\begin{Bmatrix}\sin n\theta\\ \cos n\theta\end{Bmatrix} \quad (25c)$$

The s-dependent coefficients with subscripts n on the right-hand side of (25) are governed by a system of equations which is obtained from (22) and, after using the assumption that the shell is thin,[3] can be written as

$$w_{n,s} = \frac{1}{R_\phi} u_{\phi n} - \beta_{\phi n} \quad (26a)$$

$$u_{\phi n,s} = -Uw_n - \frac{\nu\cos\phi}{r} u_{\phi n} \mp \frac{\nu n}{r} u_{\theta n} + \frac{1}{K} N_{\phi n} + \alpha(1+\nu)T_{0n} \quad (26b)$$

$$u_{\theta n,s} = \pm\frac{D\sin 2\phi}{Kr^3} w_n \pm \frac{n}{r} u_{\phi n} + \frac{\cos\phi}{r} u_{\theta n} \pm \frac{2Dn\sin\phi}{Kr^2}\beta_{\phi n} + \frac{2}{(1-\nu)K} N \quad (26c)$$

$$\beta_{\phi n,s} = -\frac{\nu n^2}{r^2} w_n \mp \frac{\nu n\sin\phi}{r^2} u_{\theta n} - \frac{\nu\cos\phi}{r}\beta_{\phi n} + \frac{1}{D} M_{\phi n} + \alpha(1+\nu)T_{1n} \quad (26d)$$

$$\begin{aligned} Q_{n,s} = {} & \frac{1-\nu}{r^4}[(1+\nu)n^4 D \\ & + 2n^2 D\cos^2\phi + (1+\nu)Kr^2\sin^2\phi]w_n \\ & + (1-\nu)\frac{\cos\phi}{r^2}\left[(1+\nu)K\sin\phi - \frac{n^2}{r}DJ\right]u_{\phi n} \\ & \pm \frac{(1-\nu)n}{r^2}\left[(1+\nu)D\frac{n^2}{r^2}\sin\phi + (1+\nu)K\sin\phi\right]u_{\theta n} \\ & + n^2(1-\nu)(3+\nu)D\frac{\cos\phi}{r^3}\beta_{\phi n} - \frac{\cos\phi}{r}Q_n + UN_{\phi n} \\ & \mp \frac{nD\sin 2\phi}{Kr^3}N_n + \frac{\nu n^2}{r^2}M_{\phi n} - p_n \mp \frac{n}{r}m_{\theta n} \\ & - \alpha(1-\nu^2)\frac{1}{r}\left(K\sin\phi\, T_{0n} + D\frac{n^2}{r}T_{1n}\right) \end{aligned} \quad (26e)$$

$$\begin{aligned} N_{\phi n,s} = {} & (1-\nu)\frac{\cos\phi}{r^2}\left[(1+\nu)K\sin\phi - \frac{n^2}{r}JD\right]w_n \\ & + \frac{1-\nu}{r^2}\left[(1+\nu)K\cos^2\phi + \frac{n^2}{2}DJ^2\right]u_{\phi n} \\ & \pm \frac{(1-\nu^2)nK\cos\phi}{r^3}u_{\theta n} - \frac{n^2(1-\nu)}{r^2}DJ\beta_{\phi n} \\ & - \frac{1}{R_\phi}Q_n - (1-\nu)\frac{\cos\phi}{r}N_{\phi n} \mp \frac{n}{r}N_n \end{aligned}$$

[3] In the derivation of the system of equations (6)–(13) the assumption is made that the shell is sufficiently thin, so that $1 + h/R_\phi \approx 1$, where R denotes the minimum principal radius of curvature. This same approximation is used to obtain the following equations from (22).

$$- p_{\phi n} - \alpha(1 - \nu^2)K \frac{\cos\phi}{r} T_{\theta n} \quad (26f)$$

$$N_{n,s} = \pm \frac{n(1-\nu)}{r^2} \left[(1+\nu)D \frac{n^2}{r^2} \sin\phi + (1+\nu)K \sin\phi \right] w_n$$
$$\pm \frac{(1-\nu^2)nK\cos\phi}{r^2} u_{\phi n} + \frac{n^2(1-\nu^2)K}{r^2} u_{\theta n}$$
$$\pm nD \frac{1-\nu}{r^2} \cos\phi \left[(1+\nu)\frac{\sin\phi}{r} - H \right] \beta_{\phi n}$$
$$\pm n \frac{\nu}{r} N_{\phi n} - \frac{2\cos\phi}{r} N_n$$
$$\pm \frac{\nu n \sin\phi}{r^2} M_{\phi n} - p_{\theta n} - \frac{\sin\phi}{r} m_{\theta n}$$
$$\mp \alpha(1-\nu^2)\frac{1}{r}\left(KT_{\theta n} + D\frac{\sin\phi}{r} T_{1n} \right) \quad (26g)$$

$$M_{\phi n,s} = n^2(1-\nu)(3+\nu)D\frac{\cos\phi}{r^3} w_n - n^2 \frac{1-\nu}{r^2} JDu_{\phi n}$$
$$\pm nD\frac{1-\nu}{r^2}\cos\phi\left[(1+\nu)\frac{\sin\phi}{r} - H\right] u_{\theta n}$$
$$+ D\frac{1-\nu}{r^2}[(1+\nu)\cos^2\phi + 2n^2]\beta_{\phi n} + Q \mp \frac{2nD\sin\phi}{Kr^2} N_n$$
$$- (1-\nu)\frac{\cos\phi}{r} M_{\phi n} - m_{\phi n} - \alpha(1-\nu^2)D\frac{\cos\phi}{r} T_{1n} \quad (26h)$$

The double signs in (26) correspond to the top or bottom trigonometric function employed in (24) and (25).

The quantities which are not included in the fundamental variables can be expressed by means of separation of variables by

$$\{N_\theta, M_\theta, Q_\phi\} = \{N_{\theta n}, M_{\theta n}, Q_{\phi n}\} \begin{Bmatrix} \cos n\theta \\ \sin n\theta \end{Bmatrix} \quad (27a)$$

$$\{N_{\theta\phi}, M_{\theta\phi}, Q_\theta\} = \{N_{\theta\phi n}, M_{\theta\phi n}, Q_{\theta n}\} \begin{Bmatrix} \sin n\theta \\ \cos n\theta \end{Bmatrix} \quad (27b)$$

where the s-dependent coefficients with subscripts n must satisfy a set of equations obtained from equations (14)–(17) and (23) in the form

$$N_{\theta n} = \nu N_{\phi n} + (1-\nu^2)\frac{K}{r^2}(w_n \sin\phi + u_{\phi n}\cos\phi \pm n u_{\theta n})$$
$$- \alpha(1-\nu^2)KT_{\theta n} \quad (28a)$$

$$M_{\theta n} = \nu M_{\phi n} + (1-\nu^2)\frac{D}{r}\left(\frac{n^2}{r} w_n + \beta_{\phi n}\cos\phi \right.$$
$$\left. \pm n\frac{\sin\phi}{r} u_{\theta n}\right) - \alpha(1-\nu^2)DT_{1n} \quad (28b)$$

$$M_{\theta\phi n} = \frac{1-\nu}{2r}\left(\mp \frac{2n\cos\phi}{r} w_n \pm nJu_{\phi n} \right.$$
$$\left. + H\cos\phi u_{\theta n} \mp 2n\beta_{\phi n}\right) + \frac{D}{K}\frac{\sin\phi}{r} N_n \quad (28c)$$

$$Q_{\theta n} = \mp \frac{n}{r} M_{\theta n} + M_{\theta\phi n,s} + \frac{2\cos\phi}{r} M_{\theta\phi n} + m_{\theta n} \quad (28d)$$

$$N_{\theta\phi n} = N_n - \frac{\sin\phi}{r} M_{\theta\phi n} \quad (28e)$$

$$Q_{\phi n} = Q_n \mp \frac{n}{r} M_{\theta\phi n} \quad (28f)$$

The double signs agree correspond to the top or bottom trigonometric function employed in (24), (25), and (27).

The remainder of this paper is concerned with the solution of the system of equations (26), subject to the boundary conditions on two edges s = const. It should be noted that after the expansion of the loads in Fourier series, the solution to (26) is obtained for each integral value of n separately, and then the solutions are superimposed to form a Fourier series expansion for the unknown variables.

Reduction to Initial Value Problems

This section is concerned with the reduction of a two-point boundary-value problem governed by

$$\frac{dy(x)}{dx} = A(x)y(x) + B(x) \quad (29a)$$

to a series of initial-value problems. In (29a), $y(x)$ is an $(m, 1)$ matrix which represents m unknown functions; x is the independent variable; $A(x)$ denotes the (m, m) coefficient matrix; and $B(x)$ is the $(m, 1)$ matrix of the nonhomogeneous terms. The elements of $A(x)$ and $B(x)$ are given piecewise continuous functions of x. The object is to determine $y(x)$ in the interval $a \le x \le b$ subject to m boundary conditions stated in terms of linear combinations of $y(a)$ and $y(b)$ in the form

$$F_a y(a) + F_b y(b) = G \quad (29b)$$

where F_a, F_b are (m, m) matrices and G is an $(m, 1)$ matrix, which are known from the statement of the boundary conditions of the problem. It should be clear that the governing system of equations (26) derived in the preceding section is stated in the form of (29a), and that the appropriate boundary conditions for a shell of revolution can be expressed in the form of (29b).

Let the complete solution of (29a) be written as

$$y(x) = Y(x)C + Z(x) \quad (30)$$

where the $(m, 1)$ matrix C represents m arbitrary constants, and $Y(x)$ is an (m, m) and $Z(x)$ an $(m, 1)$ matrix which are defined as the homogeneous and particular solutions of (29a) in the form

$$\frac{dY(x)}{dx} = A(x)Y(x) \quad (31a)$$

$$\frac{dZ(x)}{dx} = A(x)Z(x) + B(x) \quad (31b)$$

The initial conditions for determining $Y(x)$ and $Z(x)$ are

$$Y(a) = I \quad (32a)$$

$$Z(a) = 0 \quad (32b)$$

where I is the unit matrix.

Evaluation of (30) at $x = a$ leads at once, in view of (32a, b), to $C = y(a)$, and then (30) at $x = b$ can be written as

$$y(b) = Y(b)y(a) + Z(b) \quad (33)$$

Together with (29b), equation (33) constitutes a system of $2m$ linear algebraic equations from which the $2m$ unknowns, $y(a)$ and $y(b)$, are determined. Once $y(a)$ is known, the solution at any value of x is obtained from (30) provided that the values of $Y(x)$ and $Z(x)$ at that particular x are stored. This completes the reduction of a two-point boundary-value problem defined by (29) to $m + 1$ initial-value problems given by (31, 32).

As stated in the introduction, the solution for $y(b)$ obtained by means of this procedure suffers a complete loss of accuracy at some critical length of the interval. The reason for this phenomenon can be seen clearly from (33). When the initial-value problems defined by (31, 32) are solved with the use of the expre-

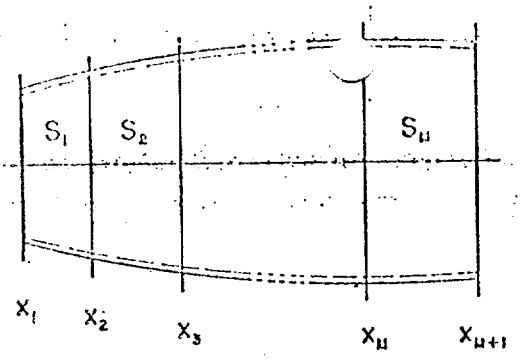

Fig. 2 Notation for division of total interval into segments

tions (26) for shells of revolution, it is observed that the elements of $Y(x)$ and $Z(x)$ increase in magnitude in such a way that if the length is increased by any factor n, then these solutions increase in magnitude approximately exponentially with n.

Consider, for example, the axisymmetric case when the deformation in the shell is caused by some prescribed edge conditions at $x = a$, say, by $M_\phi(a) = 1$ and $N_\phi(a) = Q(a) = 0$. It is reasonable to expect that the corresponding solutions at $x = b$ become smaller and smaller when the interval (a, b) is increased in length. The connection between $y(b)$ and $y(a)$ is given by the matrix equation (33) with the following magnitudes of the elements: $y(b)$-small, $Y(b)$-large, $y(a)$-unity. Clearly, the only way that the matrix product of (33) can give small values of $y(b)$ is that a number of significant digits of the large values of $Y(b)$ subtract out. When the length of the interval is increased, $Y(b)$ increase, while $y(b)$ decrease, and invariably all accuracy is lost at some critical length because all significant digits of $Y(b)$ in (33) are lost. This simple example serves as an illustration for the loss of accuracy encountered in the analysis of shells if the foregoing reduction technique is employed.

A convenient length factor, defined by

$$\beta = l[3(1 - \nu^2)]^{1/4}/(Rh)^{1/2} \tag{34}$$

where l is the length of the meridian of the shell and R is a minimum radius of curvature, can be used for an approximate estimate of the critical length of the shell. If the solutions $Y(x)$ and $Z(x)$ are obtained with a six-digit accuracy, then the foregoing procedure gives good results in the range $\beta \leq 3 - 5$.

However, the loss of accuracy of the solution can be avoided and shells of revolution with much larger values of β can be analyzed by means of the direct integration technique if the multisegment method given in the next section is employed.

Multisegment Method of Integration

Let the shell be divided into M-segments (denoted by S_i, where $i = 1, 2, \ldots, M$) of arbitrary length in each of which $\beta \leq 3$. Denote the coordinates of the ends of the segments by $x = x_i$, where the left-hand edge of the shell is at $x = x_1$ and the right-hand edge is at $x = x_{M+1}$, as shown in Fig. 2. In analogy to (30), the solution in the total interval $x_1 \leq x \leq x_{M+1}$ now can be written as

$$y(x) = Y_i(x)y(x_i) + Z_i(x) \tag{35}$$

where $Y_i(x)$ and $Z_i(x)$ denote the matrices corresponding to $Y(x)$ and $Z(x)$ in each segment $S_i(x_i \leq x \leq x_{i+1})$ and are given by

$$\frac{dY_i(x)}{dx} = A(x)Y_i(x) \tag{36a}$$

$$Y_i(x_i) = I \tag{36b}$$

$$\frac{dZ_i(x)}{dx} = A(x)Z_i(x) + B(x) \tag{36c}$$

$$Z_i(x_i) = 0 \tag{36d}$$

Requiring continuity of all elements of $y(x)$ at the points x_i, $i = 2, 3, \ldots, M + 1$, the following M-matrix equations are obtained from (35):

$$y(x_{i+1}) = Y_i(x_{i+1})y(x_i) + Z_i(x_{i+1}) \tag{37}$$

where $i = 1, 2, \ldots, M$. Equations (37) involve $M + 1$ unknown $(m, 1)$ matrices: $y(x_i)$, $i = 1, 2, \ldots, M + 1$. However, if the quantities prescribed at the edges of the shell are the fundamental variables, then the total number of unknowns is reduced by m, because $m/2$ elements of $y(x_1)$ and $m/2$ elements of $y(x_{M+1})$ are known. The same is true if the boundary conditions are stated in terms of linear combinations of the fundamental variables in the form of (29b). In this case, $y(x_1)$ and $y(x_{M+1})$ should be premultiplied by nonsingular (m, m) transformation matrices F_1 and F_{M+1}, respectively, so that the elements of the products contain the quantities prescribed at each edge. After eliminating $y(x_1)$ and $y(x_{M+1})$ from (37) by means of these products, it is concluded that (37) will retain its form if, after integration and before substitution into (37), $Y_1(x_2)$ is postmultiplied by F_1^{-1}, while $Y_M(x_{M+1})$ and $Z_M(x_{M+1})$ are premultiplied by F_{M+1}. In the following, it will be regarded that this transformation is carried out and that $y(x_1)$ and $y(x_{M+1})$ contain among their elements those quantities which are prescribed at $x = x_1$ and $x = x_{M+1}$, respectively.

Thus for all boundary conditions in the form of (29b), the system of M matrix equations (37) involves exactly M times m unknowns, and formally it can be solved by any method which is applicable to a large number of equations. However, the success of the procedure given in this paper lies in the application of Gaussian elimination directly on the matrix equations (37).

First a rearrangement of elements is performed. Since those $m/2$ elements of $y(x_1)$ and $y(x_{M+1})$ which are known through the boundary conditions can be any $m/2$ of the m-elements, it is necessary to rearrange the rows of $y(x_1)$ and $y(x_{M+1})$ so that the known elements are separated from the unknown elements. It is assumed here that the first $m/2$ elements of $y(x_1)$, denoted by $y_1(x_1)$, are known and that the last $m/2$ elements, denoted by $y_2(x_1)$, are unknown. On the other hand, $y_1(x_{M+1})$ are the unknown and $y_2(x_{M+1})$ are the known elements of $y(x_{M+1})$. Since the order of the variables in the column matrix $y(x)$ is arbitrary, it should be emphasized that this separation of elements does not involve any restriction on the boundary conditions, and that any natural boundary condition in the form of (29b) can be prescribed at each edge. The separation is achieved by a simple rearrangement of the columns of $Y_1(x_2)$ and the rows of $Y_M(x_{M+1})$ and $Z_M(x_{M+1})$ after integrating the initial-value problems defined by (36) to the ends of the segments S_1 and S_M and multiplying by F_1^{-1} and F_{M+1} as stated in the foregoing.

Once it is established which parts of $y(x_1)$ and $y(x_{M+1})$ are known, the continuity conditions (37) are rewritten as a partitioned matrix product of the form

$$\begin{bmatrix} y_1 \\ \hline y_2 \end{bmatrix}_{i+1} = \left[\begin{array}{c|c} Y_i^1(x_{i+1}) & Y_i^2(x_{i+1}) \\ \hline Y_i^3(x_{i+1}) & Y_i^4(x_{i+1}) \end{array}\right] \begin{bmatrix} y_1(x_i) \\ \hline y_2(x_i) \end{bmatrix} + \begin{bmatrix} Z_i^1(x_{i+1}) \\ \hline Z_i^2(x_{i+1}) \end{bmatrix} \tag{38}$$

so that each of the equations (37) turns into a pair of equations, given by

$$\begin{aligned} Y_i^1(x_{i+1})y_1(x_i) + Y_i^2(x_{i+1})y_2(x_i) - y_1(x_{i+1}) &= -Z_i^1(x_{i+1}) \\ Y_i^3(x_{i+1})y_1(x_i) + Y_i^4(x_{i+1})y_2(x_i) - y_2(x_{i+1}) &= -Z_i^2(x_{i+1}) \end{aligned} \tag{39}$$

The result is a simultaneous system of $2M$ linear matrix equations, in which the known coefficients $Y_i^j(x_{i+1})$ and $Z_i^j(x_{i+1})$ are $(m/2, m/2)$ and $(m/2, 1)$ matrices, respectively, and the unknowns $y_j(x_i)$ are $(m/2, 1)$ matrices. Since $y_1(x_1)$ and $y_2(x_{M+1})$ are known, there are exactly $2M$ unknowns: $y_1(x_i)$, with $i = 2, 3, \ldots, M + 1$, and $y_2(x_i)$, with $i = 1, 2, \ldots, M$.

By means of Gaussian elimination, t[illegible]stem of equations (39) is first brought to the form

$$\begin{bmatrix} E_1 & -I & 0 & 0 & 0 & 0 \\ 0 & C_1 & -I & 0 & 0 & 0 \\ 0 & 0 & E_2 & -I & 0 & 0 \\ 0 & 0 & 0 & C_2 & -I & 0 \\ 0 & 0 & 0 & 0 & E_M & -I \\ 0 & 0 & 0 & 0 & 0 & C_M \end{bmatrix} \begin{bmatrix} y_2(x_1) \\ y_1(x_2) \\ y_2(x_2) \\ y_1(x_M) \\ y_2(x_M) \\ y_1(x_{M+1}) \end{bmatrix} = \begin{bmatrix} A_1 \\ B_1 \\ A_2 \\ B_2 \\ A_M \\ B_M \end{bmatrix} \tag{40}$$

where the dots indicate the triangularized equations (39) with $i = 3, 4, \ldots, M - 1$. The $(m/2, m/2)$ matrices E_i, C_i are defined by

$$E_1 = Y_1^2 \tag{41a}$$

$$C_1 = Y_1^4 E_1^{-1} \tag{41b}$$

and for $i = 2, 3, \ldots, M$

$$E_i = Y_i^2 + Y_i^1 C_{i-1}^{-1} \tag{41c}$$

$$C_i = (Y_i^4 + Y_i^3 C_{i-1}^{-1}) E_i^{-1} \tag{41d}$$

The $(m/2, 1)$ matrices A_i, B_i are given by

$$A_1 = -Z_1^1 - Y_1^1 y_1(x_1) \tag{42a}$$

$$B_1 = -Z_1^2 - Y_1^3 y_1(x_1) - Y_1^4 E_1^{-1} A_1 \tag{42b}$$

and for $i = 2, 3, \ldots, M - 1$

$$A_i = -Z_i^1 - Y_i^1 C_{i-1}^{-1} B_{i-1} \tag{42c}$$

$$B_i = -Z_i^2 - Y_i^3 C_{i-1}^{-1} B_{i-1} - (Y_i^4 + Y_i^3 C_{i-1}^{-1}) E_i^{-1} A_i \tag{42d}$$

Finally, for the Mth segment

$$A_M = -Z_M^1 - Y_M^1 C_{M-1}^{-1} B_{M-1} \tag{42e}$$

$$B_M = y_2(x_{M+1}) - Z_M^2 - Y_M^3 C_{M-1}^{-1} B_{M-1} - (Y_M^4 + Y_M^3 C_{M-1}^{-1}) E_M^{-1} A_M \tag{42f}$$

For brevity, in place of $Y_i^j(x_{i+1})$ and $Z_i^j(x_{i+1})$, the symbols Y_i^j and Z_i^j have been used.

By means of (41) and (42), the unknowns of (39) are obtained by

$$y_1(x_{M+1}) = C_M^{-1} B_M \tag{43a}$$

$$y_2(x_M) = E_M^{-1}[y_1(x_{M+1}) + A_M] \tag{43b}$$

and for $i = 1, 2, \ldots, M - 1$

$$y_1(x_{M-i+1}) = C_{M-1}^{-1}[y_2(x_{M-i+1}) + B_{M-i}] \tag{43c}$$

$$y_2(x_{M-i}) = E_{M-i}^{-1}[y_1(x_{M-i+1}) + A_{M-i}] \tag{43d}$$

It should be noted that (41)–(43) must be evaluated in succession, because each equation involves the result obtained by the preceding equation.

Once all the unknowns $y(x_i)$ are found, the fundamental variables are determined from (35) at a[illegible] value of x at which the solutions $Y_i(x)$ and $Z_i(x)$ [illegible] stored d[illegible] the integration of the initial-value problems of [illegible]). The [illegible]tion of (36) can be accomplished by means o[illegible] [illegible]ed direct integration methods.

On the basis of the sy[illegible]) given in an earlier section and the method [illegible] in the last two sections, the author has pr[illegible] a com[illegible] program[4] which has been applied to many sh[illegible]figuratio[illegible]ving large values of β and successfully tested a[illegible]st known results. One example of a pressurized torus with β [illegible] 57 is presented in the next section.

The program admits arbitrary meridional variations, including discontinuities, in all shell parameters. It also admits ring loads in the form of prescribed values of N_ϕ, M_ϕ, N, or Q at any value of ϕ on the shell. Such loads introduce discontinuities in the solution for the corresponding stress resultants, and they can be represented at every x_i by an $(m, 1)$ discontinuity matrix which is simply added to the matrix $Z_i(x_{i+1})$ on the right-hand side of (37). This feature is of great value if shell joints are considered. Any discontinuity, either in geometry or in loads, is easily handled by requiring that the end point of a segment coincides with the location of the discontinuity. Since integration is restarted at the beginning of each segment, the precise effect of the discontinuity is obtained. The program outputs all fundamental variables at a number of desired points within each segment, and it also computes the values of $y(x_i)$ twice; once from (43) and then from (35). If a certain number of significant figures of these values match, then the continuity conditions are known to be satisfied to the same number of figures. In this way, a convenient error estimate of the solution is obtained for every case.

[4] The program was written and all calculations were carried out by the author on the IBM 709 computer at the Yale Computer Center. The direct integration of (36) is performed by means of the Adams predictor-corrector method, which selects an optimum step size at every step according to a prescribed accuracy.

Example: Pressurized Torus

In this section the stresses and displacements are determined in a complete torus subjected to a constant internal pressure. It is well known that the solution of this problem, when obtained by means of the linear membrane theory of shells, has a discontinuity in the displacement field. It has been shown by Jordan [16] and by Sanders and Liepins [17] that a satisfactory solution with regard to the displacement field for a sufficiently thin shell can be obtained if the nonlinear membrane theory of shells is employed. Subsequently, Reissner [18] established bounds on certain parameters which show when the nonlinear membrane and when the linear bending theory is applicable. It seems worthwhile to give here the solution for a pressurized torus as predicted by the linear bending theory.

The geometry of the torus is shown in Fig. 3. With regard to the quantities employed in equations (26), the two necessary parameters for a torus are given as

$$R_\phi = b \tag{44a}$$

$$r = a + b \sin \phi \tag{44b}$$

Because of symmetry with respect to the plane XX, Fig. 3, the

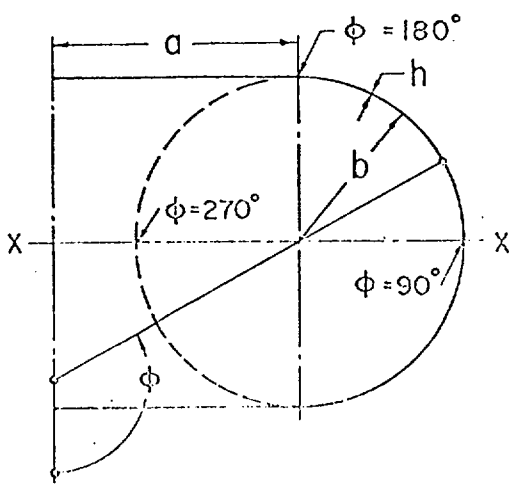

Fig. 3 Geometry of torus considered in example

Table 1 Stresses and displacements of a pressurized torus, $pb/Eh = 0.002$, $a/b = 1.5$, $\nu = 0.3$

ϕ \ h/b	$\sigma_{\phi m}/E \times 10^3$	$(\sigma_{\phi b}/E) \times 10^3$			$(w/b) \times 10^3$		
	0.005	0.05	0.02	0.005	0.05	0.02	0.005
90	1.601	−0.063	−0.031	−0.016	1.249	1.284	1.298
108	1.613	−0.188	−0.093	−0.019	1.261	1.315	1.328
126	1.650	−0.886	−0.123	−0.030	1.359	1.393	1.427
144	1.720	−1.915	−0.908	−0.020	1.786	1.597	1.625
162	1.832	−0.895	−1.378	−0.910	2.820	2.580	2.159
171	1.906	1.002	0.168	−0.605	3.467	3.493	3.297
180	1.990	3.089	2.277	1.482	3.994	4.331	4.815
184.5	2.042	3.890	3.035	1.968	4.150	4.576	5.248
189	2.104	4.270	3.119	1.520	4.208	4.637	5.151
193.5	2.175	4.178	2.580	0.530	4.156	4.509	4.693
198	2.254	3.610	1.589	−0.274	3.998	4.221	4.162
216	2.642	−0.587	−0.957	−0.079	2.652	2.527	2.481
234	3.168	−1.245	−0.291	−0.066	1.273	1.269	1.269
252	3.730	−0.717	−0.344	−0.077	0.416	0.417	0.414
270	3.997	−0.824	−0.331	−0.081	0.103	0.101	0.100

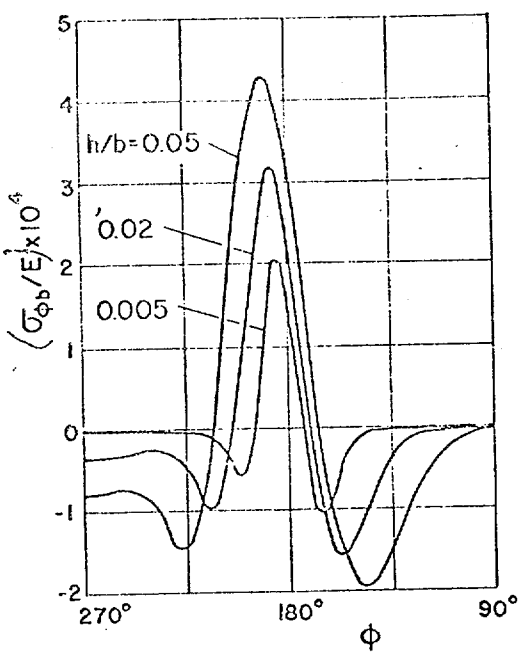

Fig. 4 Meridional bending stress $\sigma_{\phi b}$ at outer fiber versus meridional coordinate ϕ

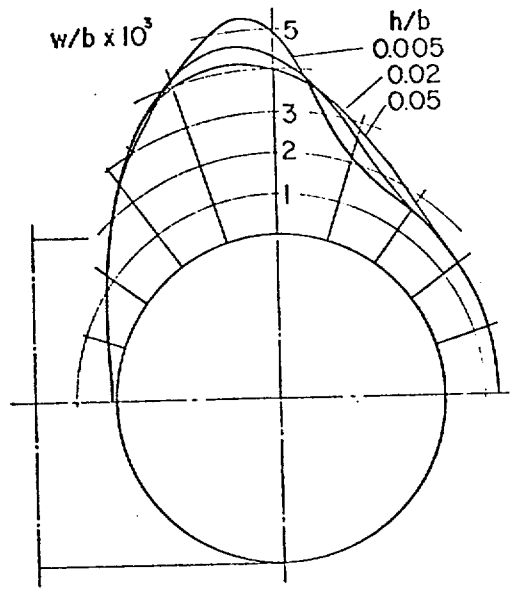

Fig. 5 Normal displacement w versus ϕ showing deformed section

integration of the initial-value problems is carried out from $\phi = 90°$ to $\phi = 270°$, and the boundary conditions at these endpoints are $u_\phi = \beta_\phi = Q = 0$. For the purpose of comparison with the results of [16] and [17], the load parameter is chosen as $pb/Eh = 0.002$ and $a/b = 1.5$.

The numerical values of the normal displacement, meridional membrane stress $\sigma_{\phi m} = N_\phi/h$, and meridional bending stress $\sigma_{\phi b} = 6M_\phi/h^2$ at $\zeta = h/2$ for a pressurized torus are shown in Table 1 and in Figs. 4 and 5. These results were taken from the output of the computer program prepared for an arbitrary shell of revolution after prescribing the geometric parameters as given by (41). The meridional membrane stress distribution agrees very well with that obtained in [17] by means of the membrane theory of shells and it shows only a small variation with h/b. The deformed shapes of the cross section of the torus shown in Fig. 5 for three values of h/b are in qualitative agreement with those given in [16] and [17], but their quantitative agreement cannot be expected because the values of h/b used in this example are outside the range where the bending effects are negligible. This is confirmed by the examination of the bending stresses shown in Fig. 4. The maximum value of $\sigma_{\phi b}$ occurs at $\phi = 189°$ for $h/b = 0.05$ and at $\phi = 184.5°$ for $h/b = 0.005$, which are also the points of maximum normal displacement and curvature as seen in Fig. 5. The comparison of the membrane and the maximum bending stresses at various values of h/b is shown in Table 2.

Table 2 Maximum meridional bending stress and meridional membrane stress at $\phi = \phi_0$

h/b	0.05	0.02	0.005
ϕ_0	189°	189°	184.5°
$(\sigma_{\phi m}/E) \times 10^3$	2.053	2.082	2.042
$(\sigma_{\phi b}/E) \times 10^3$	0.427	0.312	0.197
$100\ (\sigma_{\phi b}/\sigma_{\phi m})$	20.8	15.0	9.6

It is of significance to note that even for the thickness ratio $h/b = 0.005$, which for many applications would be regarded as small, the maximum bending stress is about 10 percent of the membrane stress at the same point. Such effects of bending in a torus were previously noted by Clark [19], and they are also in agreement with the statement made by Goldenveizer [20] that when the middle surface touches a closed-plane curve, which in a torus corresponds to $\phi = 180°$, then in the vicinity of this curve bending stresses should be expected and the membrane theory is not applicable.

The boundary layer shown in Fig. 4 is also in agreement with the conclusions reached in [18] to the effect that when μ and ρ given by

$$\mu = [12(1 - \nu^2)]^{1/2}(b/a)(b/h)$$

$$\rho = 12(1 - \nu^2)(p/E)(b/h)^3$$

are large compared to unity, then a boundary layer in the neighborhood of $\phi = 180°$ should be anticipated. For the present example, μ ranges from 44 to 440 and ρ from 9 to 871. However, since p is the only load parameter of the problem, the solutions shown in Figs. 4 and 5 are proportional to p, and the boundary layer remains unaffected if p alone is varied. Of course, for very large values of p the deformation of the torus may exceed the limits of a linear theory which according to [18] restrict ρ to the range $\rho \ll \mu^{1/2}$.

Acknowledgments

This research has been supported by the National Science Foundation Grant #23922. Many ideas leading to this paper originated from the consulting work performed by the author for the United Technology Center, Sunnyvale, California. The author wishes to thank the staff of the Applied Mechanics Department of UTC for many illuminating discussions concerning this subject.

References

1 P. M. Naghdi and C. N. DeSilva, "Deformation of Elastic Ellipsoidal Shells of Revolution," *Proceedings of the Second U. S. National Congress of Applied Mechanics*, 1954, pp. 333–343.

2 W. Lohmann, "Beitrag zur Integration der Reissner-Meissnerschen Schalengleichung für Behälter unter konstantem Innerdruck," *Ingenieur-Archiv*, vol. 6, 1935, pp. 338–346.

3 H. Münz, "Ein Integrationsverfahren für die Berechnung der Biegespannungen achsensymmetrischer Schalen unter achsensymmetrischer Belastung," *Ingenieur-Archiv*, vol. 19, 1951, pp. 103–117, 255–270.

4 E. Klingbeil, "Zur Theorie der Rotationsschalen vom Standpunkt numerischer Rechnungen," *Ingenieur-Archiv*, vol. 27, 1959, pp. 242–249.

5 G. D. Galletly, W. T. Kyner, and C. E. Moller, "Numerical Methods and the Bending of Ellipsoidal Shells," *Journal of the Society of Industrial and Applied Mathematics*, vol. 9, 1961, pp. 489–513.

6 R. K. Penny, "Symmetric Bending of the General Shell of Revolution by Finite Difference Method," *Journal of Mechanical Engineering Science*, vol. 3, 1961, pp. 369–377.

7 P. P. Radkowski, R. M. Davis, and M. R. Bolduc, "Numerical Analysis of Equations of Thin Shells of Revolution," *American Rocket Society Journal*, vol. 32, 1962, pp. 36–41.

8 W. K. Sepetoski, C. E. Pearson, I. W. Dingwell, and A. W. Adkins, "A Digital Computer Program for the General Axially Symmetric Thin-Shell Problem," JOURNAL OF APPLIED MECHANICS, vol. 29, TRANS. ASME, vol. 84, Series E, 1962, pp. 655–661.

9 B. Budiansky and P. P. Radkowski, "Numerical Analysis of Unsymmetrical Bending of Shells of Revolution," *AIAA Journal*, vol. 1, 1963, pp. 1833–1842.

10 J. E. Goldberg and J. L. Bogdanoff, "Static and Dynamic Analysis of Nonuniform Conical Shells under Symmetrical and Unsymmetrical Conditions," *Proceedings of the Sixth Symposium on Ballistic Missile and Aerospace Technology*, Academic Press, New York, N. Y., vol. 1, 1961, pp. 219–238.

11 C. R. Steele, "Shells of Revolution With Edge Loads of Rapid Circumferential Variation," JOURNAL OF APPLIED MECHANICS, vol. 29, TRANS. ASME, vol. 84, Series E, 1962, pp. 701–707.

12 R. D. Schile, "Asymptotic Solution of Nonshallow Shells of Revolution Subjected to Nonsymmetric Loads," *Journal of the Aerospace Sciences*, vol. 29, 1962, pp. 1375–1379.

13 E. Reissner, "A New Derivation of the Equations for the Deformation of Elastic Shells," *American Journal of Mathematics*, vol. 63, 1941, pp. 177–184.

14 S. A. Ambartsumyan, "Theory of Anisotropic Shells" (in Russian), *Gosudarstvennoye Izdatel'stvo Fiziko-Matematicheskoi Literatury*, Moscow, USSR, 1961, p. 91.

15 P. M. Naghdi, "On the Theory of Thin Elastic Shells," *Quarterly of Applied Mathematics*, vol. 14, 1957, pp. 369–380.

16 P. F. Jordan, "Stresses and Deformations of the Thin-Walled Pressurized Torus," *Journal of the Aerospace Sciences*, vol. 29, 1962, pp. 213–225.

17 J. L. Sanders, Jr., and A. Liepins, "Toroidal Membrane Under Internal Pressure," *AIAA Journal*, vol. 1, 1963, pp. 2105–2110.

18 E. Reissner, "On Stresses and Deformations in Toroidal Shells of Circular Cross Section Which Are Acted Upon by Uniform Normal Pressure," *Quarterly of Applied Mathematics*, vol. 21, 1963, pp. 177–187.

19 R. A. Clark, "On the Theory of Thin Elastic Toroidal Shells," *Journal of Mathematics and Physics*, vol. 29, 1950, pp. 146–178.

20 A. L. Goldenveizer, *Theory of Elastic Thin Shells*, Pergamon Press, New York, N. Y., 1961, p. 480.

Reprinted from September 1964 issue
of the Journal of Applied Mechanics.

APPENDIX B

EXTRACT FROM REPORT GAMD-7445
PRESENTING BASIS FOR CRITICALITY ANALYSES

SUMMARY OF INITIAL CRITICALITY EXPERIMENT FOR TORREY PINES TRIGA MARK III REACTOR STARTUP

Introduction

The reactor is a movable core water reflected reactor using standard stainless steel clad fuel elements containing 8.5 weight-percent uranium with 20% enrichment. The hydrogen-zirconium ratio is 1.65 to 1.0. A detailed description and safety analysis for the reactor is given in GA-5400, Rev. B.

Initial Criticality

On January 19, 1966 the reactor was loaded to criticality with 56 fuel elements plus 4 fuel followers. The inverse multiplication data is shown in Table 1 and the loading sequence is shown in Figure 1 and in Table 2.

Figures 2, 3, 4 and 5 show the inverse multiplication data for the four instrumentation channels. Because of their low sensitivity the ion chambers did not respond until a number of fuel elements were loaded.

The instrumentation used for the startup included one fission counter, one BF_3 counter and two gamma compensated neutron sensitive ion chambers.

The fuel was loaded to give the most compact core possible, that is, the fuel elements with the highest uranium loading were placed in the center of the core. The average uranium loading in the core for initial criticality was 8.52 wt. %

Neutron Instrumentation

The standard reactor instrumentation for the startup and post-startup tests consisted of two gamma compensated neutron sensitive ion chambers which provided information to log and linear reactor power channels. A fission counter which supplied startup data at low power levels and an uncompensated gamma ion chamber which was used for power indication at high reactor power levels. The compensated ion chambers were mounted above the reactor core over the E, F and G rings. These two chambers were located at opposite sides of the core. The fission and gamma chambers were also

located above the core over the F and G ring region. Figure 9 indicates the relative position of these four reactor power sensing devices.

Table 1

Multiplication Data

Core Configuration	FC cts/min.	FC M	FC 1/M	BF_3 CB/min.	BF_3 M	BF_3 1/M
1. All rods up	290	-	-	48	-	-
2. 30 elements all rods up	467	1.64	0.609	808	16.8	0.0594
a. Reg DN	439	1.51	0.660	682	14.2	0.0703
b. Safe DN	452	1.55	0.640	583	12.1	0.0823
c. Shim I DN	427	1.47	0.679	587	12.2	0.0817
d. Shim II DN	442	1.52	0.656	670	13.9	0.0716
3. 45 elements all rods up	610	2.10	0.475	5733	119.4	0.00837
a. Reg DN	765	2.63	0.379	3226	67.2	0.0148
b. Safe DN	832	2.86	0.348	3554	74.0	0.0135
c. Shim I DN	658	2.26	0.440	2960	61.6	0.162
d. Shim II DN	824	2.84	0.351	4401	91.6	0.0109
4. 46 elements all rods up	832	2.86	0.348	6314	131.5	0.00760
5. 51 elements all rods up	2898	9.99	0.100	17333	361.1	
a. Reg DN	1539	5.30	0.188	6769	141.0	0.00709
b. Safe DN	1845	6.36	0.157	7835	163.2	0.00612
c. Shim I DN	1153	3.97	0.251	5639	117.4	0.00851
d. Shim II DN	1597	5.50	0.181	7781	162.1	0.00616
6. 52 elements all rods up	3373	11.63	0.0859	23833	496.4	0.00201
7. 53 elements all rods up	4574	15.77	0.0634	37000	770.8	0.00129
8. 54 elements all rods up	7284	25.11	0.0398	66100	1377	0.000726
9. 55 elements all rods up	19936	68.81	0.0145	194000	4041	0.00247
10. 56 elements all rods up	on 25 sec period					

Fuel element in A ring.

Table 2

Loading Sequence

Grid Position	Fuel Element No.	U-235 in Element	% U	Total U-235 in Core Excluding Fuel Followers	No. of Elements In-core
First Loading					
A-1	3922	38	8.52	38	1
B-1	4061	39	8.75	77	2
B-2	4084	39	8.71	116	3
B-3	4049	39	8.70	155	4
B-4	4110	39.	8.75	194	5
B-5	4100	40	8.75	234	6
B-6	4121	39	8.70	273	7
C-1	4053	39	8.69	312	8
C-2	4113	39	8.55	351	9
C-3	4068	39	8.69	390	10
C-4	4092	39	8.62	429	11
C-5	4118	39	8.60	468	12
C-6	4091	39	8.58	507	13
C-7	4076	39	8.69	546	14
C-8	3672	39	8.61	585	15
C-9	4123	39	8.68	624	16
C-10	4102	39	8.53	663	17
C-11	4070	39	8.64	702	18
C-12	4050	39	8.64	741	19
D-1	4066	38	8.45	779	20
D-2	4109	38	8.50	817	21
D-4	4072	38	8.52	855	22
D-7	4060	38	8.42	893	23
D-9	4058	38	8.51	932	24
D-10	4055	39	8.58	970	25
D-11	4057	38	8.47	1008	26
D-13	4111	38	8.45	1046	27
D-15	4120	39	8.54	1085	28
D-16	4125	38	8.44	1123	29
D-18	4063	38	8.49	1161	30
Second Loading					
D-6	4062	38	8.47	1199	31
D-5	4083	39	8.59	1238	32
E-6	4119	38	8.42	1276	33
E-7	3677	38	8.42	1314	34
E-8	4054	38	8.41	1352	35
E-3	4081	38	8.45	1390	36
E-4	4080	38	8.41	1428	37
E-5	4103	38	8.43	1466	38
E-2	4046	39	8.49	1505	39
E-1	3679	38	8.42	1543	40
E-24	3683	38	8.40	1581	41
E-23	3854	38	8.49	1619	42
E-22	4077	38	8.42	1657	43
E-21	3855	38	8.49	1695	44
E-20	4090	39	8.56	1734	45

Grid Position	Fuel Element No.	U-235 in Element	% U	Total U-235 in Core Excluding Fuel Followers	No. of Elements In-core
Third Loading					
E-17	4089	38		1772	46
Fourth Loading					
D-14	4071	39	8.50	1811	47
E-19	4105	38	8.40	1849	48
E-18	3675	38	8.33	1887	49
E-16	3673	38	8.32	1925	50
E-15	4082	38	8.47	1963	51
Fifth Loading					
E-9	3680	38	8.36	2001	52
Sixth Loading					
E-10	3682	38	8.36	2039	53
Seventh Loading					
E-11	3685	38	8.44	2077	54
Eighth Loading					
E-12	3671	38	8.33	2115	55
Ninth Loading					
E-13	3684	38	8.43	2153	56

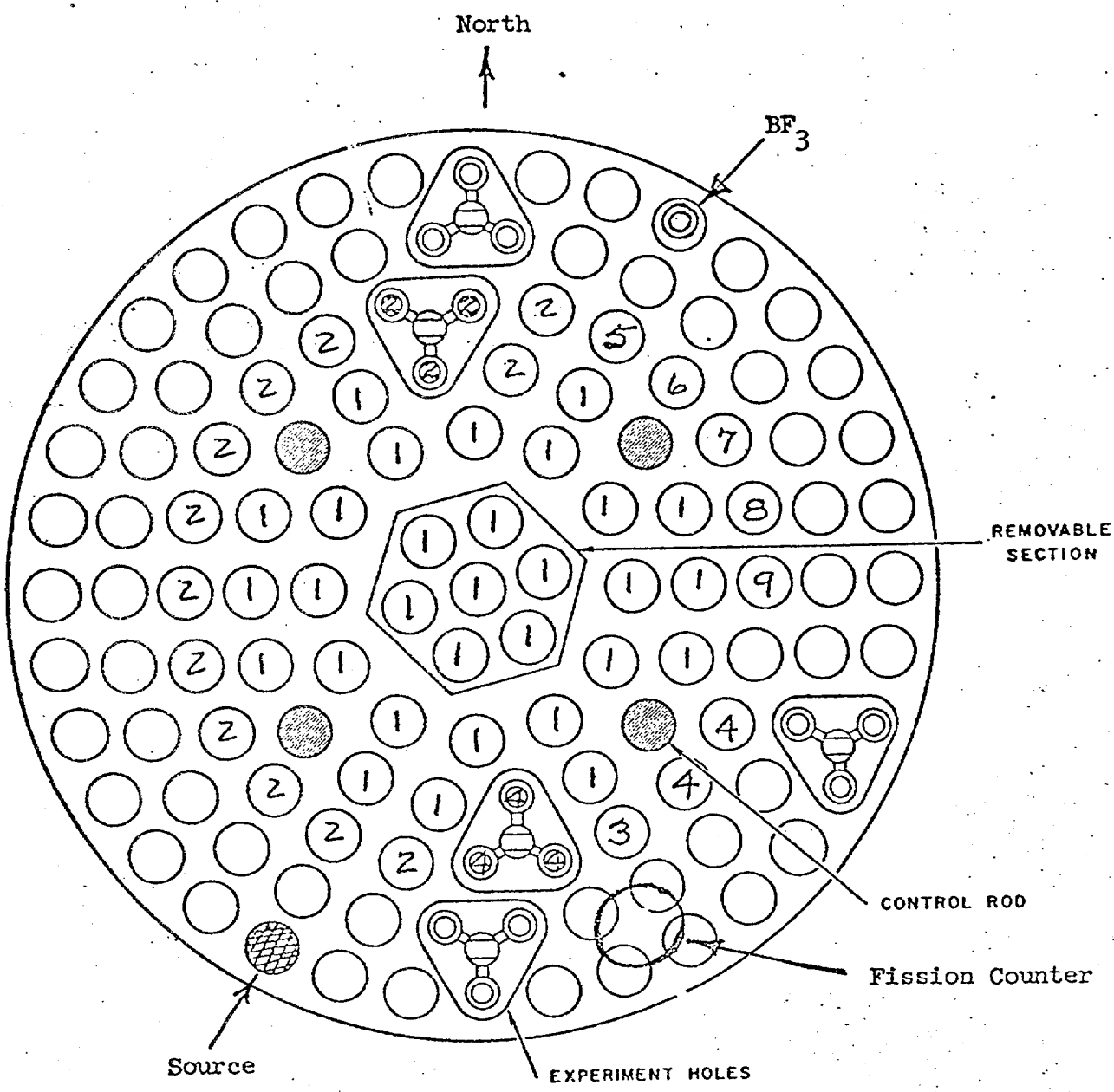

Fig. 1 - Critical loading sequence

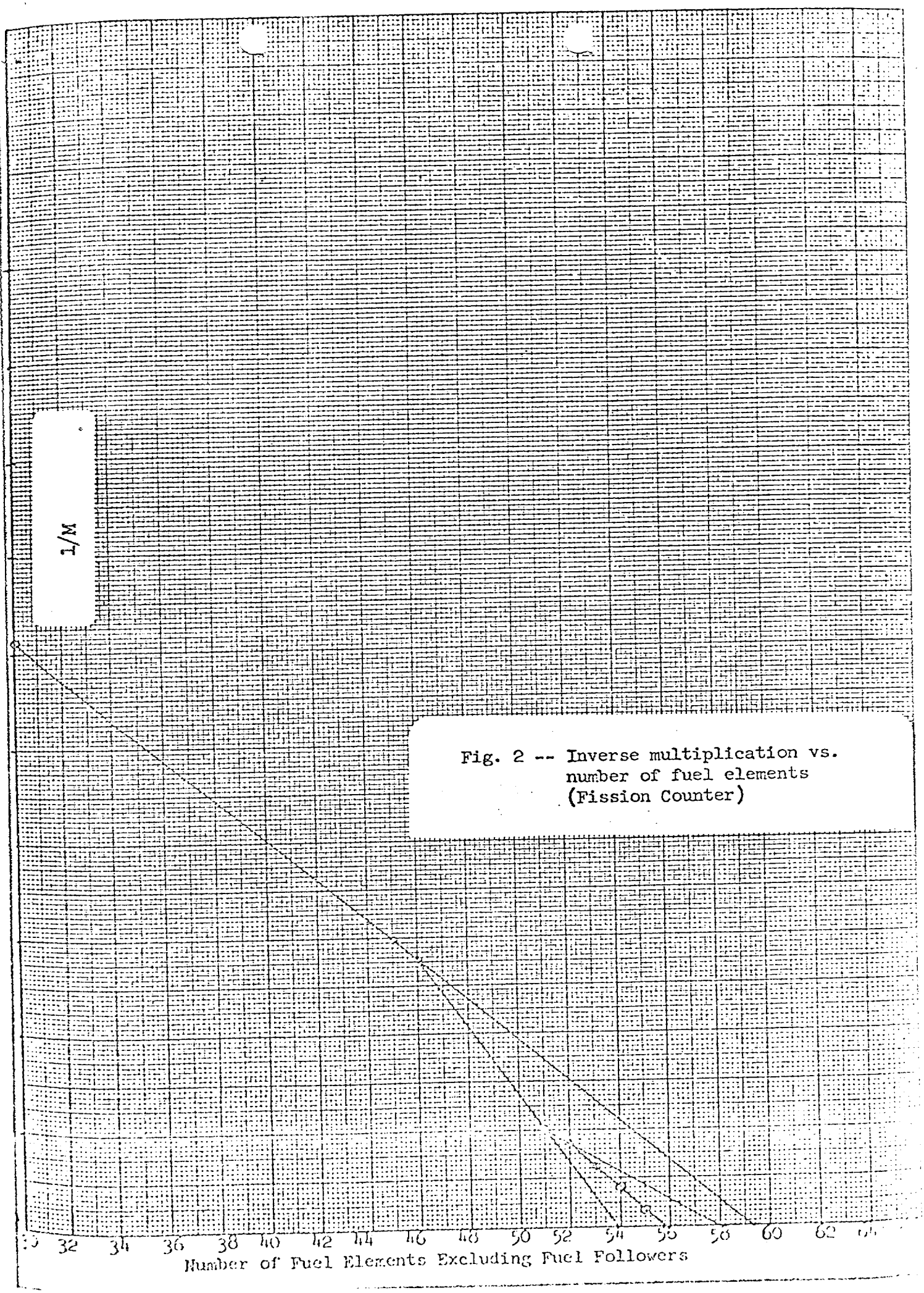

Fig. 2 -- Inverse multiplication vs. number of fuel elements (Fission Counter)

Fig. 3 -- Inverse multiplica n vs. number of fuel elements (BF_3 Counter)

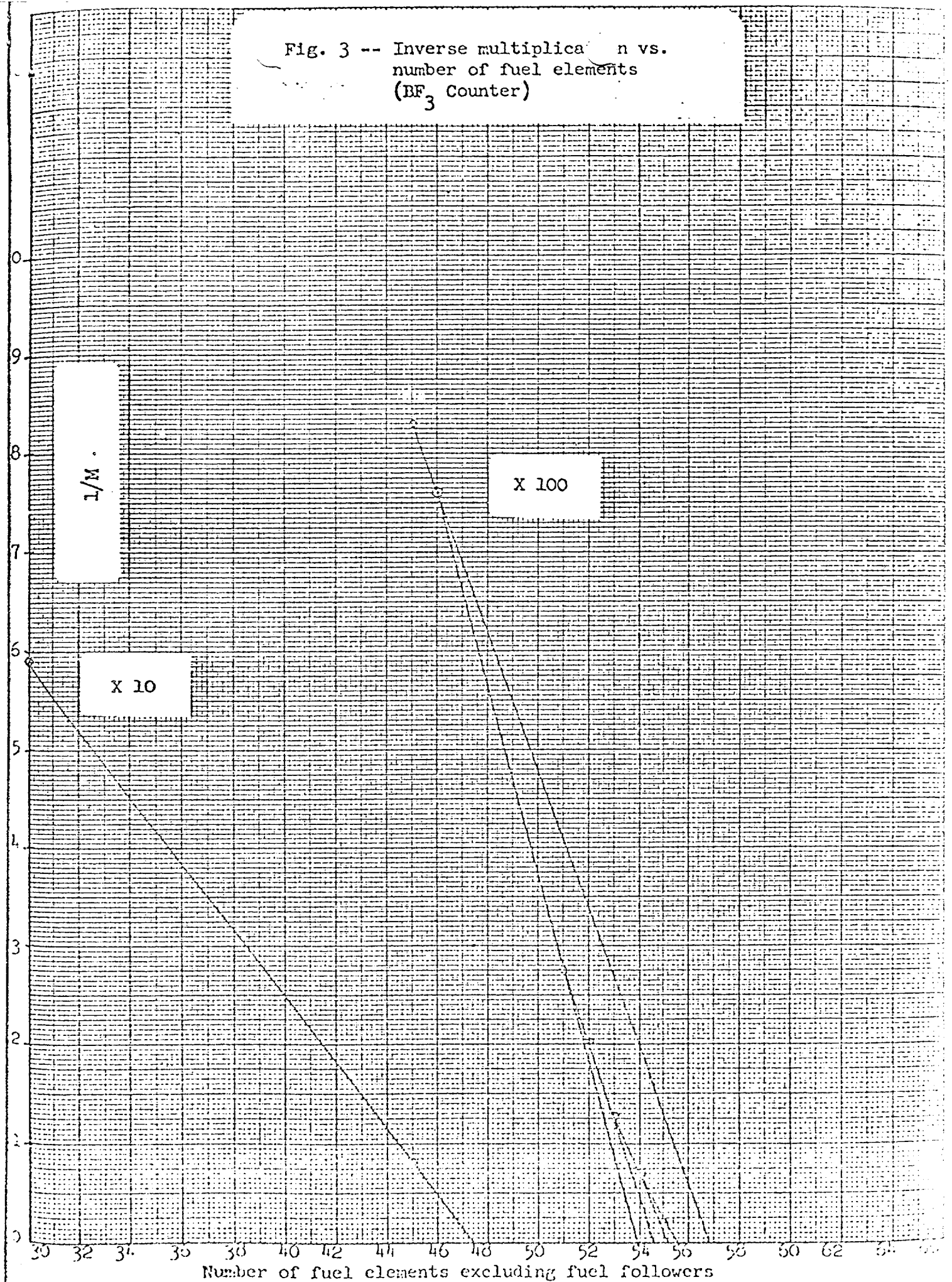

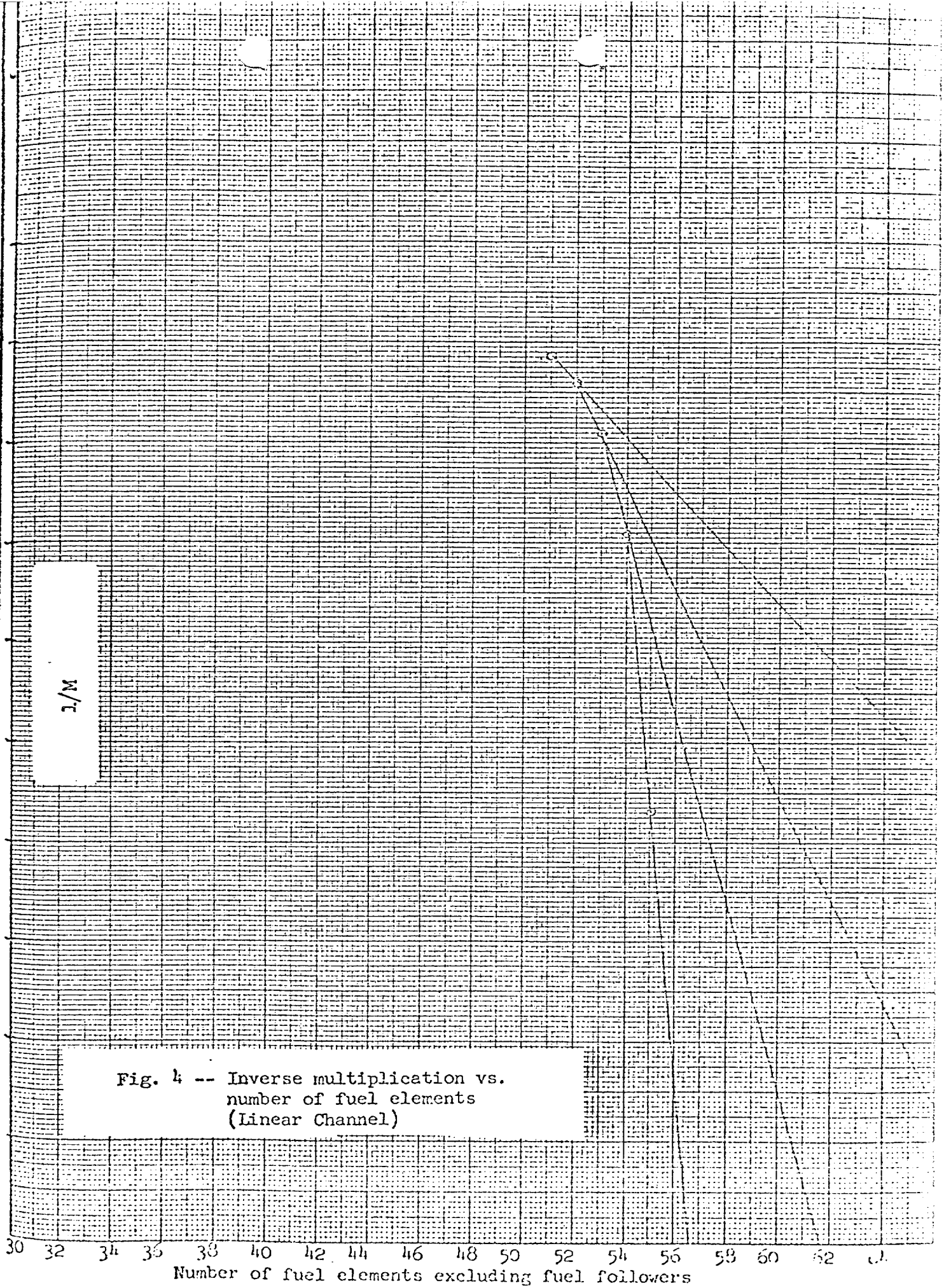

Fig. 4 -- Inverse multiplication vs. number of fuel elements (Linear Channel)

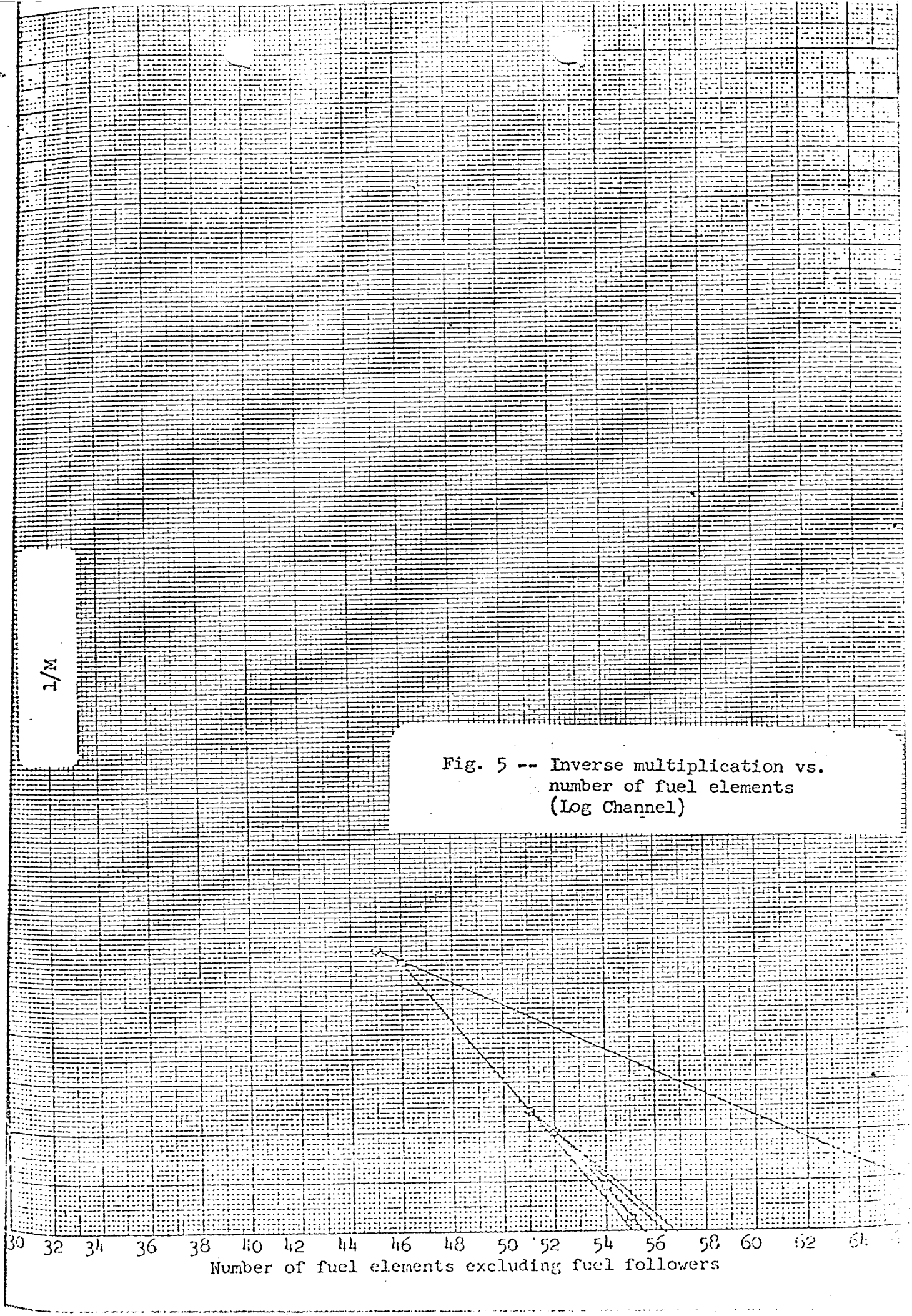

Fig. 5 -- Inverse multiplication vs. number of fuel elements (Log Channel)

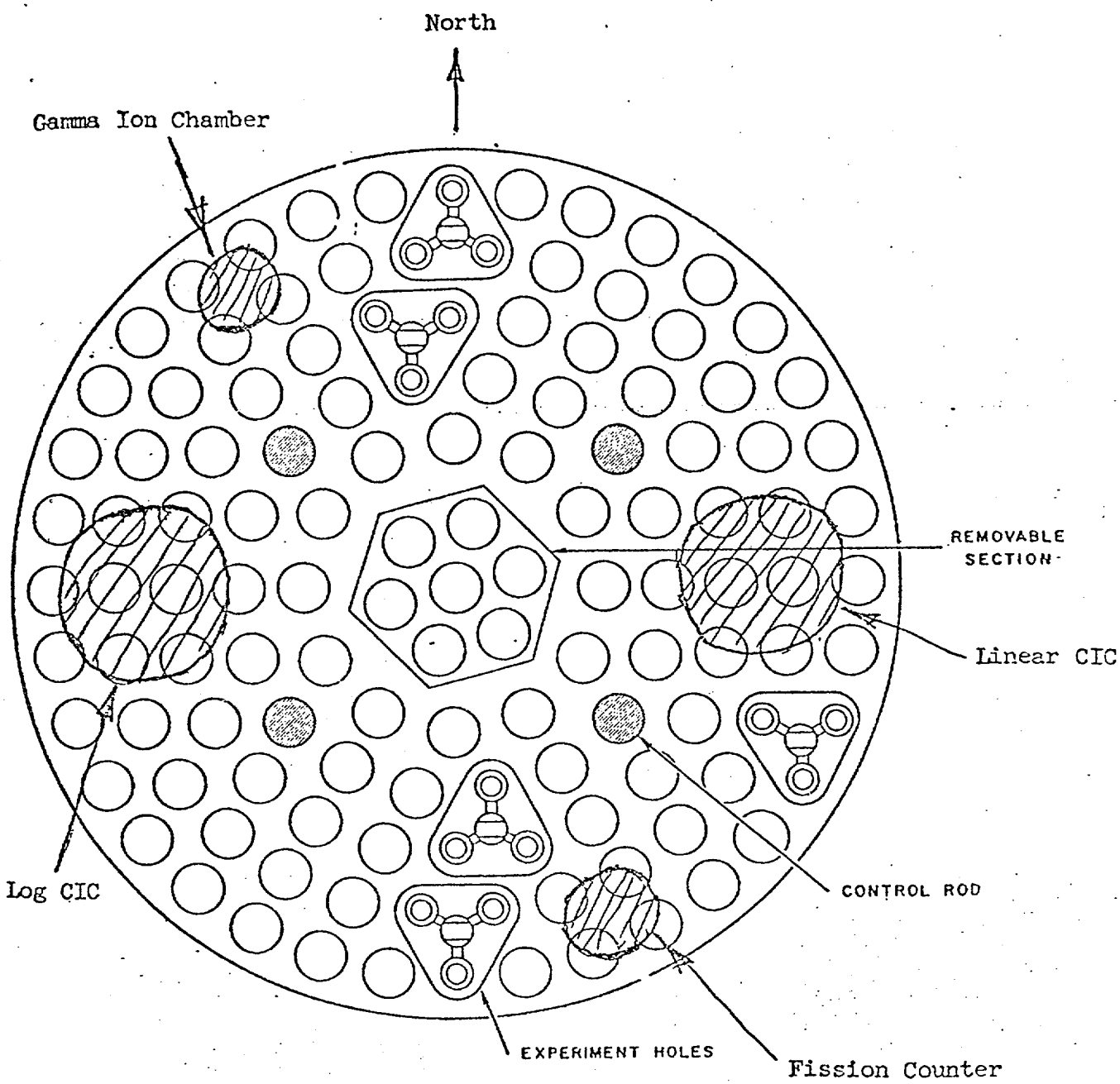

Fig. 9 - Location of instrumentation